

Review

Solution-processable polymeric solar cells: A review on materials, strategies and cell architectures to overcome 10%



Ikerne Etxebarria, Jon Ajuria, Roberto Pacios *

IK4-ikerlan, Goiru Kalea, 20500 Arrasate, Spain
CIC microGUNE, 20500 Arrasate, Spain

ARTICLE INFO

Article history:

Received 4 November 2014

Received in revised form 8 January 2015

Accepted 9 January 2015

Available online 28 January 2015

Keywords:

Organic photovoltaics

Single cells

Tandem cell

Processes

Layout

ABSTRACT

Organic photovoltaics will become 30 years old relatively soon. In spite of the impressive development achieved throughout these years, especially in terms of reported power conversion efficiencies, there are still important technological and fundamental obstacles to circumvent before they can be implemented into reliable and long-lasting applications. Regarding device processing, the synthesis of highly soluble polymeric semiconductors first, and fullerene derivatives then, was initially considered as an important breakthrough that would definitely change the fabrication of photovoltaics once for all. Nowadays, the promise of printing solar cells by low-cost and high throughput mass production techniques still stands. However, the potential and the expectation raised by this technology is such that it is considerably difficult to keep track of the most significant progresses being now published in different and even monographic journals. There is therefore the need to compile the most remarkable advances in well-documented reviews than can be used as a reference for future ideas and works. In this letter, we review the development of polymeric solar cells from its origin to the most efficient devices published to date. After analyzing their fundamental limits, we separate these achievements into three different categories traditionally followed by the scientific community to push devices over 10%

Abbreviations: BCP, bathocuproine; BHJ, bulk heterojunction; $C_2C_6GeIDT-BT$, germanium heteroatom substituted indacenodithiophene-benzothiadiazole; Ca, calcium; C-PCBSD, cross-linked [6,6]-phenyl- C_{61} -butyric styryl dendron ester; Cs_2CO_3 , cesium carbonate; CsF, cesium fluoride; DIO, 1,8-diiodooctane; DTS(FBTTh₂)₂, 7,7'-[4,4-bis(2-ethylhexyl)-4H-silolo[3,2-b:4,5-b']dithiophene-2,6-diyl]bis[6-fluoro-4-(5'-hexyl-[2,2'-bithiophen]-5-yl)benzo[c][1,2,5]thiadiazole]; F-DTS, p-DTS(FBTTh₂)₂; E_g , energy bandgap; FF, fill factor; HOMO, highest occupied molecular orbital; ICBA, 1',1'',4',4''-tetrahydro di[1,4]methanonaphthaleno[1,2:2',3',5,6:6',2',3''] [5,6] fullerene- C_{60} ; I_{sc} , short circuit current; ITO, indium tin oxide; J_{sc} , short circuit current density; LiAc, lithium acetate; LiF, lithium fluoride; LUMO, lower unoccupied molecular orbital; MDMO-PPV, poly[2-methoxy-5-(3',7'-dimethyloctyloxy)-1,4-phenylenevinylene]; MEH-PPV, poly[2-methoxy-5-(2'-ethyl-hexyloxy)-p-phenylenevinylene]; MgF, magnesium fluoride; MoO₃, molybdenum oxide; NiO, nickel oxide; NREL, national renewable energy laboratory; ODT, 1,8-octanedithiol; OLED, organic light emitting diode; OPV, organic photovoltaics; P3HT, poly(3-hexylthiophene); P3HTTz, poly(3-hexyl-2,5-bithienyl); pBBTDPP2, poly[3,6-bis-(4'-dodecyl-[2,2']bithiophenyl-5-yl)-2,5-bis-(2-ethyl-hexyl)-2,5-dihydropyrrolo[3,4-]pyrrole-1,4-dione]; PBDTTPD, poly(benzo[1,2-b:4,5-b']dithiophene-thieno[3,4-c]pyrrole-4,6-dione); PBDTTT-C-T, poly[4,8-bis(5-(2-ethylhexyl)thiophen-2-yl)-benzo[1,2-b:4,5-b']dithiophene-2,6-diyl-alt-(4-(2-ethylhexanoyl)-thieno[3,4-b]thiophene-)-2,6-diyl]; PC₆₀BM, [6,6]-phenyl-C₆₁-butyric acid methyl ester; PC₇₀BM, [6,6]-phenyl C₇₁-butyric acid methyl ester; PCDTBT, poly N-9-hepta-decanyl-2,7-carbazole-alt-5,5,4,7-di-2-thienyl-2,1,3-benzothiadiazole; PCE, Power conversion efficiency; PCPDTBT, poly[2,6-(4,4-bis-(2-ethylhexyl)-4H-cyclopenta [2,1-b:3,4-b']dithiophene)-alt-4,7(2,1,3-benzothiadiazole)]; PDPP3T, poly[2,5-bis(2-hexyldecyl)-2,3,5,6-tetrahydro-3,6-dioxopyrrolo[3,4-c]pyrrole-1,4-diyl]-alt-2,2':5',2''-terthiophene]-5,5''-diyl]; PDPP-TPT, poly-2,5-bis(2-hexyldecyl)-2,3,5,6-tetrahydro-3,6-dioxopyrrolo[3,4-c]pyrrole-1,4-diyl]-alt-(2,2'-(1,4-phenylene)bisthiophene)-5,5'-diyl]; PDPP-TT-T, thieno[3,2-b]thiophene-diketopyrrolopyrrole; PDTP-DFBT, poly[2,7-(5,5-bis-(dimethyloctyl)-5H-dithieno[3,2-b:2',3'-d]pyran)-alt-4,7-(5,6-difluoro-2,1,3-benzothiadiazole)]; PEDOT:PSS, poly(3,4-ethylenedioxythiophene) poly(styrenesulfonate); PEIE, polyethylenimine, 80% ethoxylated; PFN, poly[(9,9-bis(3'-(N,N-dimethylamino)propyl)-2,7-fluorene)-alt-2,7-(9,9-dioctylfluorene)]; PIDTDTQx, indacenodithiophene-quinoxaline; P_{in} , incident light intensity; PMDPP3T, poly[[2,5-bis(hexyldecyl)-2,3,5,6-tetrahydro-3,6-dioxopyrrolo[3,4-c]pyrrole-1,4-diyl]-alt-[3',3''-dimethyl-2,2':5',2''-terthiophene]-5,5''-diyl]; PPV, poly(p-phenylenevinylene); PTB7, poly[[4,8-bis[(2-ethylhexyl)oxy]benzo[1,2-b:4,5-b']dithiophene-2,6-diyl][3-fluoro-2-[(2-ethylhexyl)carbonyl]thieno[3,4-b]thiophenediyl]]; R2R, roll-to-roll; TiO_x, titanium oxide; V₂O₅, vanadium oxide; V_{oc} , open circuit voltage; WO₃, tungsten trioxide; ZnO, zinc oxide; ZnS, zinc sulfide.

* Corresponding author.

E-mail address: rpacios@ikerlan.es (R. Pacios).<http://dx.doi.org/10.1016/j.orgel.2015.01.014>

1566-1199/© 2015 Elsevier B.V. All rights reserved.

power conversion efficiency: Active materials, strategies -fabrication/processing procedures- that can mainly modify the active film morphology and result in improved efficiencies for the same starting materials, and all the different cell layout/architectures that have been used in order to extract as high photocurrent as possible from the Sun. The synthesis of new donors and acceptors, the use of additives and post-processing techniques, buffer interlayers, inverted and tandem designs are some of the most important aspects that are in detailed reviewed in this letter. All have equally contributed to develop this technology and leave it at doors of commercialization.

© 2015 Elsevier B.V. All rights reserved.

0. Broader context

Organic photovoltaics (OPV) was born as a new possibility to decrease the fabrication cost of solar devices and be validated as one of the most promising renewable energy sources. Thirty years later they have still however not fulfilled this expectative. The non-stop development of existing technologies makes it still difficult for OPV to compete with traditional systems such as silicon solar cells in terms of efficiency and reliability. However, the unique selling properties of this technology extend the potential of OPV from particular niche markets to generic energy production. These are mainly based on mechanical flexibility, transparency and processing of arbitrary shape devices. In this way, OPV is still a real and promising alternative for certain applications for which added functionality to already existing elements is the key selling point. Portable/flexible/wearable electronics and building integrated photovoltaics are some of the most significant examples toward where this technology is being addressed. Moreover, the possibility of printing modules at production speeds up to several meters per second with low-cost and high throughput techniques such as inkjet, slot die, screen or gravure printing allows the coating of the same photoactive area in a single day as that of a traditional silicon foundry in a year. Thus, OPV is also a technology subject to further study for on and off-grid applications for which energy production is still the leitmotif.

1. Introduction

Abundance of raw material, simplicity in device fabrication and easy integration into different applications thanks to their lightweight, semitransparency, flexibility and color tunability, have become organic photovoltaics (OPV) into an attractive source of green energy. Nowadays research on this technology is in one way focused on understanding the physics behind and in the other way on achieving as high efficiency as possible.

Nelson calculated the limiting efficiency for an ideal single solar cell as a function of the semiconductor bandgap taking into account the incident and extracted power from the photon fluxes. She considered a two band system for which the ground state -lower band- is initially full and the excited state -upper band- is empty. The bands are separated by a bandgap, E_g , and electrons in each band are supposed to be in a quasi thermal equilibrium at the

ambient temperature. In the case that no potential is lost through resistance anywhere in the circuit, and being radiative recombination of electrons with energy larger than the bandgap the only unavoidable loss, a limiting efficiency of about 33% at a bandgap of 1.4 eV (885 nm) [1] was calculated providing all incident light with energy larger than the bandgap is absorbed. Each absorbed photon generates exactly one electron-hole pair and excited charges are completely separated. In principle, all the assumptions made for this model are perfectly valid also for organic semiconductors. However, more accurate models explicitly developed for polymer:fullerene bulk heterojunction solar cells and that hence take into account their detailed work mechanisms predict maximum efficiencies of around 15% [2] and 21% [3] for single and tandem cells respectively. The main reasons why ideal performances are not achieved are incomplete absorption of the incident light due to either reflection and/or non perfectly opaque contacts, non-radiative recombination of photogenerated carriers, i.e. excited charges that are trapped at defect sites and recombine before being collected leading to transport losses, and voltage drop due to non-ideal series and/or parallel resistance within the bulk and between the active film and the external circuit. All these aspects need to be tackled in order to overcome the current reported record efficiencies and take them closer to the theoretical limits. As we will show, this can be done by actuating on active materials, fabrication/processing procedures (strategies) and device layout/architectures.

Let us first consider the key performance characteristics of an organic solar cell and the influence of the later issues on their performance. The efficiency is defined as the ratio between the voltage at open circuit conditions (V_{oc}), the output current at short circuit conditions (I_{sc}), the fill factor (FF) of the device and the incident light intensity (P_{in}) (see Eq. (1)).

$$\eta = \frac{V_{oc} \cdot I_{sc} \cdot FF}{P_{in}} \quad (1)$$

It is clear that maximizing the efficiency is thus a matter of increasing V_{oc} , I_{sc} and FF as much as possible.

V_{oc} is ideally limited by the energy difference between the LUMO level of the acceptor and the HOMO level of the donor, therefore, it can be theoretically adjusted up to a certain extent by modifying the energy levels of the materials [4–7]. In consequence, the election of the donor and acceptor material will define the upper limit. However,

V_{oc} is not strictly an active material issue. Sub-optimal contacts can lead to either resistive losses -series resistances- and/or current leakage -parallel resistance- that might cause a voltage drop. Therefore, device engineering and cell layout are also important to guarantee large V_{oc} . This is usually achieved with the use of interlayers as we will in detail describe in Section 4.

A high photocurrent (I_{sc}) can be also achieved by selecting materials with absorption spectra that overlap the photon flux density and hence the incident power spectrum from the Sun. Even though photons with less energy than E_g are not absorbed -and do not contribute to the photocurrent-, and photons with energy greater than E_g deliver only a fraction of electrical energy to the load, the available power from these cells represents the best compromise between absorption and power delivery. As mentioned above, ideal bandgaps for photovoltaic conversion are in the red, near infra-red, part of the electromagnetic spectrum. The so called low bandgap (LBG) polymers are synthesized with this purpose [8,9]. However, as in the previous case, obtaining a high I_{sc} is not only a matter of the active material. Given the short exciton diffusion length and the relatively slow mobilities measured for most polymers, the morphology of the film is crucial in order to ensure efficient charge generation and transport processes [10]. Different fabrication/processing procedures can lead to substantially different film morphologies even when the same active materials are used. These will be detailed in Section 3. Blends of solvents, the use of additives, manual manipulation of the deposition temperature and the creation of a solvent saturated atmosphere are some of the strategies most commonly used in order to obtain a better control of the film drying process and manipulate the resulting bulk-in morphology [11–18]. In this way, it is possible to achieve ideal spatial distributions of connected electron and hole favorable domains with sizes in the order of the exciton diffusion length that guarantee efficient charge separation and transport.

The FF is the most meaningful and sensitive parameter in the characterization of solar cells since it contains information of all the processes involved in charge recombination, transport and collection. The morphology of the film

will therefore also have a direct effect in the measured FF. As commented above, deliberate manipulation of the film morphology also results in enhanced FF and device performance. Despite alternative fabrication/processing procedures, a spatial asymmetry that helps create a gradient in charge density can be beneficial to obtain selective charge injection/extraction, reduce leakage current and charge recombination and improve charge transport. The use of buffer layers has been in this way demonstrated to improve contact selectivity and device rectification. Hence, improved FF are usually measured as a consequence of modifying device layout/architectures.

Finally, materials with complementary absorption spectra can be stacked together in the same tandem device. This is an alternative device layout/architecture approach in order to maximize the light harvesting and adjust the overall absorption of the cell to the solar irradiance spectrum [19,20].

Table 1 summarizes how we can deliberately actuate on the key characteristics of organic solar cells in order to improve the overall device efficiency with the strategies reviewed in this letter: Materials, fabrication/processing procedures and device layout/architectures. All these will be in detailed analyzed in the following sections.

2. Materials

During the 80s the use of organic materials for photovoltaic devices resulted in very low efficiencies, typically below 0.1%. It was not until 1986 when Tang reported the first organic solar cell with an efficiency of 1% thanks to the combination of a donor and acceptor material [21]. Later on, the exciton dissociation rate was enhanced with the discovery by Sariciftci et al. of the charge transfer phenomenon from the MEH-PPV polymer to a highly electron accepting molecule, namely buckminsterfullerene C_{60} [22,23]. They demonstrated that fullerene strongly assists charge separation and extraction processes. However, due to the low diffusion coefficient of generated excitons in every photoactive film of these bilayer architecture devices, the low photocurrent achieved was still limiting the power conversion efficiency (PCE). Thus, the efficiency

Table 1
Summary of the key parameters for the improvement of device efficiency.

	V_{oc}	I_{sc}	FF
Active materials	<ul style="list-style-type: none"> – Low HOMO donor – High LUMO acceptor 	<ul style="list-style-type: none"> – LBG polymers: <i>Increase light absorption</i> 	<ul style="list-style-type: none"> – Balanced (fast) intrinsic e^- and h^+ mobility
Strategies: Fabrication/processing procedures	<ul style="list-style-type: none"> – Buffer interlayers: <ul style="list-style-type: none"> • Optimal contacts • Ohmic contacts 	Nanomorphology: <ul style="list-style-type: none"> – Additives – Solvent mixtures – Solvent annealing – Slow drying – Surface modification → e.g. with methanol – Thermal treatments 	
Device layout/architectures	<ul style="list-style-type: none"> – Tandem cells in series 	<ul style="list-style-type: none"> – Buffer interlayers <ul style="list-style-type: none"> • Optimal optical interference • Interfacial dipoles – Inverted devices <ul style="list-style-type: none"> • Ohmic contact – Tandem cells in parallel 	<ul style="list-style-type: none"> – Buffer interlayers <ul style="list-style-type: none"> • Contact selectivity • Interfacial dipoles • Device rectification – Inverted devices <ul style="list-style-type: none"> • Vertical segregation

of organic solar cells was considerably enhanced with the synthesis of soluble fullerene derivatives and the use of bulk heterojunction (BHJ) architecture devices [23–28]. In the latter, the electron donating polymer and the electron accepting fullerene are simultaneously solved in the same solution. The film is processed from that solution resulting in an active film with multiple donor/acceptor interfaces, analogous to the p/n interfaces in traditional semiconductors, where charges are generated after photoexcitation.

After the success of the bulk heterojunction concept, with an interpenetrating network providing a 3D structure enhancing exciton splitting and charge transfer, new approaches continued increasing the efficiency of organic photovoltaics technology. Thus, in 2001 and 2002 new record efficiencies were reported using MDMO-PPV as a new donor material [29,30]. Despite the success obtained with these materials, the large bandgap and low mobility of PPV-like polymers limited power conversion efficiencies to 3%. Efforts were focused toward new materials with optimized optoelectronic properties, like for example polythiophenes.

Polythiophenes are one of the most widely used polymers in the fabrication of organic solar cells due to the good optical and electrical properties and good thermal and chemical stability that they present. Polythiophenes are based on repeating units of thiophenes (see Fig. 1a) where different side chains can be added in order to modify the resulting properties [31,32]. Poly(3-hexylthiophene) (P3HT) (Fig. 1b) has an optical bandgap of 1.9 eV. In literature, typical efficiency values of around 3.5–4% have been achieved by several groups when combining with the fullerene derivative [6,6]-phenyl-C61-butyric acid methyl ester (PC₆₀BM) as electron acceptor [33]. However, higher efficiencies close to 4.5% have been reported when samples with higher regio-regularity [34] and/or [6,6]-phenyl C71-butyric acid methyl ester (PC₇₀BM) instead of PC₆₀BM are used.

P3HT has been for many years the standard absorber material used in organic photovoltaics. In spite of its moderate power conversion efficiency, its acceptable hole

mobility, long stability, processability and scalability make it a potential candidate for the mass-fabrication of modules using roll-to-roll (R2R) compatible deposition techniques [35,36]. One main drawback is the low V_{oc} (~0.6 V) obtained when blended with PCBM. Thiophene-thiazole (P3HTTz) copolymers (see Fig. 1c) have been synthesized with the objective of lowering the HOMO level of the donor and increase thus the V_{oc} . Combinations of these materials with fullerene derivatives as ICBA have reported V_{oc} closer to 1 V [37] which makes them promising candidates to replace P3HT as the wide bandgap polymer in tandem cells.

However, their restricted absorption to below 600 nm limits their efficiency to also below 5%. Some of the most promising candidates that are being synthesized nowadays to enhance the light harvesting include carbazole-benzothiadiazole copolymers [38–40], diketopyrrolopyrrole (DPP) based copolymers [41,42], benzodithiophene (BDT) derivatives [43–45] as well as indacenodithiophene (IDT) based copolymers [46]. This new generation of semiconducting copolymers combine electron rich segments with electron deficient units such as DPPs along the polymer backbone. The selection of different electron rich comonomers such as thiophene, fluorene or carbazole based units amongst others, determines the optical bandgap, the energy levels and the carrier mobility of the resulting copolymer. These low bandgap donor-acceptor polymers present energy gaps in the range of 1.3–1.6 eV enabling light absorption in the near-infrared region which combined with a fullerene derivative are able to extend the absorption of the organic solar cell also to the UV/Visible.

Following, some promising copolymers based in previously mentioned units will be analyzed.

2.1. Polymeric donors

It is difficult to summarize the development of all the new conjugated polymers that are being currently synthesized for polymeric solar cells. All of them are based on the conjugation of electron donating (D) and deficient units (A)

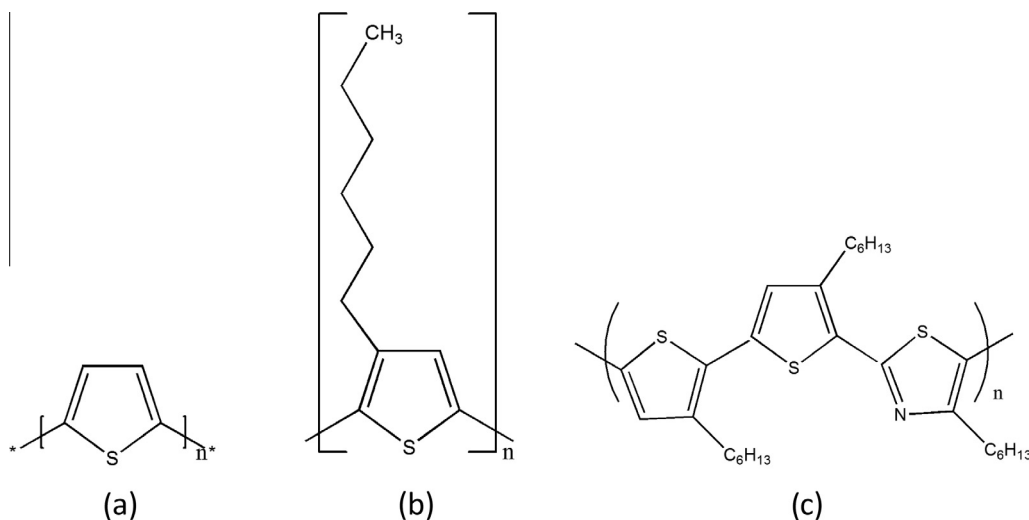


Fig. 1. Molecular structure of: (a) a polythiophene repeat unit, (b) P3HT and (c) P3HTTz.

to result in very complex D–A copolymerized structures. Following the structure used at the beginning of the section, we will use a chronological order based on the most meaningful compound part that gives name to the copolymer family and the thereof development achieved by substituting any particular moiety in terms of improving efficiency.

2.1.1. Poly carbazoles

The electron donating nitrogen unit of the central fused pyrrole ring makes carbazoles electron rich compounds. The solubility of the polymer is ensured by functionalization of the central nitrogen with an alkyl chain (see molecular structure in Fig. 2). Since carbazole derivatives present good thermal and photochemical stability and high charge mobility, they are promising candidates to be incorporated in polymers for photovoltaic applications [32,47,48].

The conjugation of the carbazole (electron donating unit) to a benzothiadiazole moiety (electron deficient unit) through a thiophene bridge gives rise to a material known as PCDTBT, see Table 2a. In combination with PC₇₀BM as acceptor, organic solar cells with power conversion efficiencies over 6% have been achieved by several groups [49–51]. These numbers can be improved to 7.2–7.5% by using advanced interface materials and antireflection coatings [38,52].

2.1.2. Dithiophene–benzothiadiazoles

A slightly different approach has been attempted by conjugating the benzothiadiazole moiety to a dithiophene unit instead of a carbazole one. The result is a polymer known as PCPDTBT (see Table 2b for the molecular structure). Organic solar cells with efficiencies up to 5.5% are usually reported for this polymer when it is blended with PC₇₀BM [53]. Moreover, by introducing a Fluor atom in this molecule (see Table 2c) that lowers the polymer HOMO level increasing thus the V_{oc} , efficiencies of 6.16% have been also achieved [54].

2.1.3. Dithienopyran–fluorobenzothiadiazoles

A further modification of this copolymer with two fluor atoms at the benzothiadiazole unit gives rises to a difluorobenzothiadiazole (DFBT) moiety that is further conjugated to a dithienopyran (DTP) segment instead of a single dithiophene. The result is a copolymer known as PDTP-DFBT (Table 2d) with efficiencies in single devices over 8% [55] with also an outstanding performance in tandem configuration as we will see in Section 4.3. A more developed semi-crystalline version known as PPDT2FBT

(Table 2e) forms a well-distributed nano-fibrillar networked morphology with the fullerene that results in balanced hole and electron mobility and tight interchain packing. Relatively thick films of around 300 nm yield record efficiencies of 9.4% [40].

2.1.4. Diketopyrrolopyrroles

Some other promising absorbers for OPV applications are copolymers based on electron deficient diketopyrrolopyrrole units. The copolymerization of this electron deficient unit with different electron rich segments have result in solar cells with efficiencies up to 8% [41,56–64].

The most promising candidates consist in the conjugation of the DPP moiety to a thienothiophene fragment with a varying number of interconnecting thiophene units. For the simplest case, Meager et al. reported PDPP-TT-T based devices with efficiencies over 7% for some particular alkyl chain branching position manipulation (see Table 2f for the molecular structure) [65]. Hendriks et al. also reported efficiencies over 7% by conjugating the DPP segment to different oligothiophenes (nT). The best material from this series (HD-PDPP3T, see Table 2g) uses terthiophene as co-monomer and reaches 7.1%. Higher efficiencies of 7.4% have been also achieved by alternating the DPP unit with thiophene–phenylene–thiophene (TPT) segments -PDPP-TPT- (Table 2h) due to the improvement in the polymerization reaction. Finally, the highest reported efficiency of 8% for a DPP based polymer has been obtained by combining these segments with a terthiophene unit in order to produce a terpolymer called PDPP3TaltTPT, Table 2i [64].

2.1.5. Benzodithiophenes

Copolymers based in the alternation of the electron donating benzodithiophene and electron deficient thieno[3,4-b]thiophene units, are also promising absorbers for organic solar cell applications. The thieno[3,4-b]thiophene units stabilize the quinoidal structure of the backbone reducing thus the energy gap of the polymer to 1.6 eV estimated from the onset of the solid state absorption (775 nm). The ester substituted thieno[3,4-b]thiophene instead, makes the polymer soluble and oxidative stable while the rigid backbone ensures a good mobility of holes [66,67].

Liang et al. developed several copolymers known as PTBs for which efficiencies up to 7.4% have been achieved by using PTB7 as the absorber (see molecular structure in Table 2j) together with PC₇₀BM as the electron acceptor for conventional configuration devices. This material is also a good example to illustrate that improving the

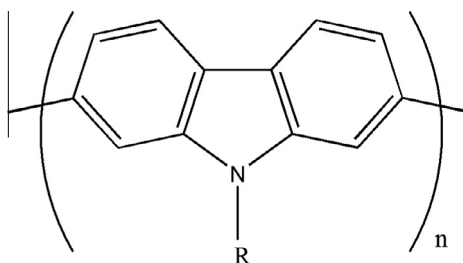


Fig. 2. Molecular structure of 2,7-carbazole.

Table 2

Highest reported efficiencies for different polymers in single devices.

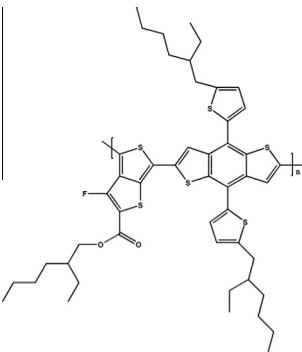
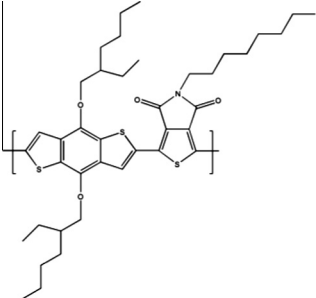
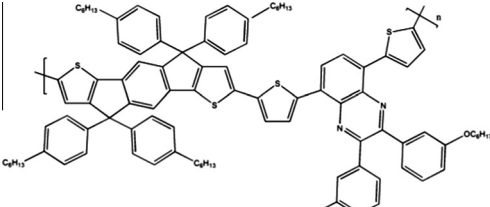
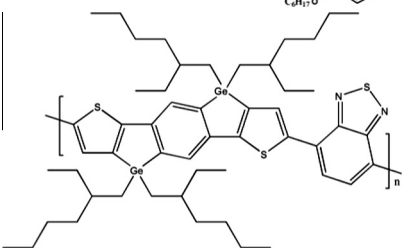
	Polymer	Record PCE	Molecular structure
(a)	PCDTBT	7.5% [52]	
(b)	PCPDTBT	5.5% [53]	
(c)	F-PCPDTBT	6.16% [54]	
(d)	PDTP-DFBT	8.1% [55]	
(e)	PPDT2FBT	9.4% [40]	
(f)	PDPP-TT-T	7.17% [65]	
(g)	HD-PDPP3T	7.1% [64]	

(continued on next page)

Table 2 (continued)

	Polymer	Record PCE	Molecular structure
(h)	PDPP-TPT	7.4% [64]	
(i)	PDPP3TaltTPT	8% [64]	
(j)	PTB7	9.2% [69]	
(k)	PBDTTT-C-T	8.3% [72]	
(l)	PBDT-TS1	9.5% [45]	

Table 2 (continued)

	Polymer	Record PCE	Molecular structure
(m)	PTB7-Th	10.1% [70]	
(n)	PBDTTPD	8.5% [73]	
(o)	PIDTDTQx	7.5% [46]	
(p)	C ₂ C ₆ GeIDT-BT	6.5% [78]	

efficiency of an organic solar cell is not only a matter of the active material. Different processing procedures and cell layouts/architectures as those being described in this review have taken the efficiency from 6.22% to 9.2%. Even though all these approaches will be in detail commented later, it is worth summarizing here the development achieved with this material by using these alternative strategies. Devices processed from a single solvent -o-dichlorobenzene (ODCB)- initially gave 6.2% PCE and FF of 60%. With different processing conditions consisting in the use of additives, in this case 1,8-diiodooctane (DIO), devices reached 7.4% and FFs of 69% [67]. He et al. changed the cell layout/architecture and were able to improve the efficiency to 8.24% with the use of a new interlayer -PFN- that it is believed to form an interfacial dipole

at the polymer/electrode interface to help charge extraction from the absorbing film [68]. Furthermore, with an additional modification of the cell layout consisting in inverting the polarity of the cell and the use of a different interlayer at the top (MoO₃), they finally reach 9.2% [69]. Standard PTB7 was latterly modified by incorporating the 2-(2-ethylhexyl)-thienyl group into the BDT unit of PTB7 to produce PTB7-Th (Table 2k). Incorporating deterministic aperiodic nanostructures (DANs) based on nanoimprint technology on PTB7-Th:PC₇₁BM has resulted in the most efficient single device reported to date with PCE of 10.1% [70].

Huo et al. also designed and synthesized an interesting thiophene-substituted benzodithiophene copolymer with carboxyl-substituted thieno[3,4-b]thiophene, PBDTTT-C-T,

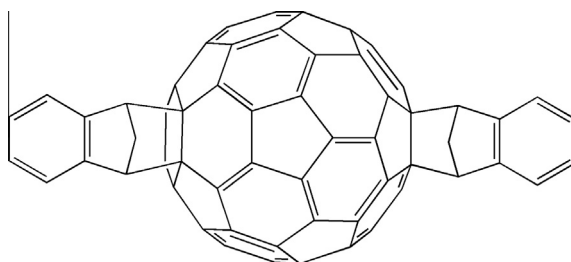


Fig. 3. Molecular structure of indene- C_{60} bis-adduct (ICBA).

that exhibits good thermal stability and hole mobility (see molecular structure in Table 2i). Devices based on PBDTTT-C-T:PCBM processed from ODCB and 3% DIO, resulted in efficiencies of 7.6% [71]. This efficiency has been recently pushed up to 8.3% by Adhikary et al. when the cell was exposure to UV-ozone [72]. Ye et al. introduced linear alkylthio chains in the BDT-T unit to produce another PBDTTT-based copolymer known as PBDT-TS1, Table 2m) from which record devices of up to 9.48% were obtained [45].

2.1.6. Thieno-pyrrole-dione benzodithiophenes

A parallel approach conjugated the electron donating benzodithiophene fragment to electron deficient thieno[3,4-c]pyrrole-4,6-dione (TPD) units to result in a copolymer known as PBDTTPD (see Table 2n). Devices based in this polymer in combination with PC₇₀BM reached PCE values up to 8.5% and V_{oc} as high as 0.97 V [73].

2.1.7. Indacenodithiophenes

Indacenodithiophenes (IDT) based copolymers have also resulted in high efficiency organic solar cells, reporting values over 7% [46,74,75]. Two cyclopentadiene rings are fused to a benzene in order to form the indaceno unit. This is later joined to a dithiophene fragment to make the IDT moiety that can be afterwards conjugated to different structures in order to obtain a new family of copolymers. These copolymers generally show high solar flux harvesting, high hole mobility and deep HOMO energy levels resulting in devices with V_{oc} values up to 0.9 [76,77]. Guo et al. developed a copolymer by conjugation of the IDT unit to quinoxaline, reporting efficiencies over 7.5% for devices based on this copolymer (PIDTDTQx:PC₇₀BM, see molecular structure in Table 2o) [46]. Similarly, Fei et al. copolymerized the IDT segment to a benzothiadiazole structure. By heteroatom substitution at the cyclopentadiene rings by either silicon or germanium, they also published efficiencies over 6.5% for C₂C₆GeIDT-BT based devices (see Table 2p) [78].

Table 2 summarizes the highest recorded PCE values for the polymers described previously and the corresponding molecular structure.

2.2. New acceptors

Acceptors are also of crucial importance in the improvement of device efficiency. Initially, mainly due to the lack of sufficiently developed soluble alternatives to evaporated C₆₀, also conjugated polymers were used as electron

acceptors. Efficient charge generation was demonstrated for hole accepting and electron accepting networks of poly-fluorene related materials [79,80] as well as for those based on poly-phenylenevinylenes [24,25]. However, charge transport was the factor limiting device performance. Nowadays, almost all reported cells with remarkable efficiencies employ soluble fullerene derivatives as electron acceptor. Amongst them, PC₆₀BM and PC₇₀BM are the most widely used. Although PC₇₀BM generally yields larger photocurrents thanks to an enhanced absorption in the visible with respect to PC₆₀BM and more favorable interpenetration properties [81], both of them have the same LUMO values which considerably limit the V_{oc} of operating devices.

A new n-type fullerene derivative, indene- C_{60} bis-adduct (ICBA) (see Fig. 3 for the molecular structure) was demonstrated to be a good alternative acceptor. ICBA has a higher LUMO level (−3.74 eV) in comparison to either PC₆₀BM or PC₇₀BM that leads to a higher V_{oc} . In this way, P3HT based devices with ICBA as an acceptor resulted in cells with V_{oc} values of 0.84 V and enhanced PCE of 6.5% [82,83].

Cheng et al. also reported P3HT based inverted solar cells using ICBA as an acceptor with a V_{oc} of 0.82 V and a PCE of 4.8%. Further improvement was carried out by the incorporation of a cross-linked fullerene derivative inter-layer, C-PCBSD, resulting in the following configuration: ITO/ZnO/C-PCBSD/ICBA:P3HT/PEDOT:PSS/Ag. The incorporation of C-PCBSD increased the photocurrent from 10.6 mA cm^{−2} to 12.4 mA cm^{−2} and the FF from 55% to 60%, and thus pushed up the PCE to 6.2% [84]. The high-quality fullerene-based organic-organic ICBA/C-PCBSD contact is believed to improve the electrical coupling at the interface. This results in a lowered contact resistance that favors the electron transport from the active layer to the cathode. Charge recombination losses at the interface are reduced and hence the overall device performance is enhanced.

Many other fullerene derivatives as bisadducts [5], diphenylmethanofullerenes (DPMS) [85], dimethylphenylmethano fullerene bisadducts [86] and endohedral fullerenes [87,88] are also being synthesized and tested in the search for large V_{oc} devices based on internal bulk polymer:fullerene heterojunction systems. In spite of these advances in the synthesis of new fullerenes, and even though soluble C₇₀ derivatives on average yield a 10% increase in photocurrent in comparison to C₆₀ ones thanks to a slightly increased absorption in the visible, the lack of a stronger absorption in the visible and in the infrared still

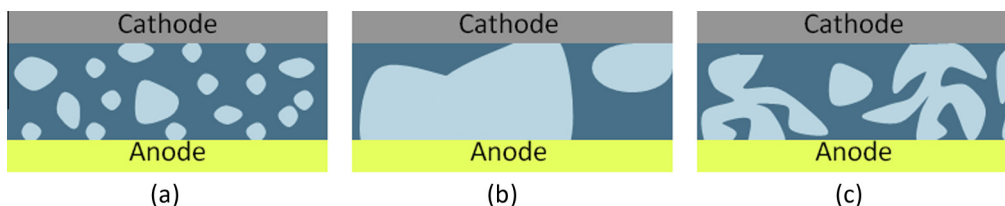


Fig. 4. Bulk heterojunction devices with different nanomorphologies: (a) small domains with a large number of interfaces: Large charge generation yield (high J_{sc}) but non efficient charge transport (low FF) due to recombination, (b) excessively large domains with a lower interface area between the donor and acceptor: Low charge generation yield (low J_{sc}) but good charge transport (high FF) and (c) intermediate domain size with an optimized interface area: Large charge generation yield (high J_{sc}) and good charge transport (high FF).

hinders further developments in achieving higher conversion efficiencies. Non fullerene containing heterojunction thin films can overcome these shortcomings [89,90]. For these materials, the morphology can be tuned with side chain modification. Also the energy levels can be modified through choice of co-couple units due to the well distributed frontier molecular orbitals. A recent work by Li et al. combined a thiazole containing DPP (with low-lying energy levels, high electron mobility and broad absorption) with a second DPP as the donor to report an efficiency of 2.9% [91]. Amongst other promising candidates are diimides derivatives as naphthalene diimide–selenophene copolymers [92] and dithienocoronene diimide based conjugated polymers [93] for which similar efficiencies as those reported for fullerenes have been obtained in combination with benchmark donor polymers. Mori et al. have recently reported an impressive 5.73% efficient polymer:polymer blend solar cell with an EQE approaching 60% [94]. They used a benzodithiophene named as PTB7-Th as electron donor. This incorporates the 2-(2-ethylhexyl)-thienyl group into the BDT unit of the well-known photovoltaic polymer, PTB7. A copolymer based on naphthalene diimide (NDI) and bithiophene moieties was used as the acceptor polymer. A very efficient charge carrier generation and collection were found to be the main reason for the superior device performance. In addition, also triimides derivatives, as a decacyclene triimide, have been incorporated in devices with some of the donors commented in the previous section as P3HT, PCDTBT and PBDTTPD [95]. Even though for this case, the reported efficiencies are still below to those obtained specially with PC₇₀BM, they are paving the way for all polymer solar cells, cutting in this way the dependence on fullerene acceptors.

3. Strategies: Fabrication/processing procedures

The morphology of the film in BHJ solar cells is a critical parameter to control the exciton dissociation rate, optimize charge transport, minimize bulk recombination, maximize the photocurrent and hence enhance the efficiency of the device [96]. On the one hand, a large amount of donor/acceptor interfaces is required in order to dissociate a large number of photogenerated excitons. On the other hand, the domain size of each material phase and interconnection between them is also important for an efficient charge transport to the corresponding electrodes. Therefore an optimum balance between the interface area,

domains size and interconnection is required to result in efficient BHJ solar cells [13].

This is schematically represented in Fig. 4. The three different morphologies depicted there are estimated to have the same overall area for both phases: Donor or polymeric and acceptor or fullerene. In Fig. 4a, the domains are excessively small and not connected with each other. Assuming adequate energy levels for both materials and efficient light absorption and exciton generation, the exciton dissociation rate is large and many free charges will be generated. However, due to the lack of connected domains, generated charges will be confined to move within the corresponding phase, leading to non-geminate recombination with charges of the opposite sign traveling through the neighboring phase. Most of the generated charges will recombine before reaching the electrodes and will not contribute to the photocurrent. In Fig. 4b, the dissociation rate will be considerably reduced due to short diffusion length of excitons and the smaller interface area. Many photogenerated excitons will not find an interface where to dissociate within their limited diffusion length of around 10–20 nm and will recombine geminately. However, most of the generated free charges that survived geminate recombination will be efficiently collected at the corresponding electrodes. They travel across their most favorable phase and do not face charges of opposite sign on their way. Therefore, a critical balance between the previously described case a and b is necessary in order to have both, efficient charge dissociation and efficient charge transport (Fig. 4c). Providing this is the case, the thickness of the film can be increased to maximize the light harvesting. Otherwise, thicker films will not yield higher efficiencies.

Solvent annealing, slow drying and thermal annealing are few examples of how to deliberately influence in the nanomorphology of the polymeric film [11–15]. Additionally, the use of additives and different solvent mixtures has also been recently demonstrated as an easy and efficient approach to modify and control the morphology of the photoactive layer [16–18,56].

3.1. Bulk morphology control: The use of additives and solvent mixtures

The use of additives and blend of solvents are very common approaches to act on bulk morphology. Both are used for the generation of a more favorable nanomorphology for the transport of electrons and holes and therefore

enhancing the final efficiency of the device. Even though they may have the same final effect, there are important differences in the working mechanisms behind these two techniques. In a solvent mixture, the polymer as well the fullerene show acceptable solubility in both components. Additives, however, show a preferable solubility for one of the active materials (usually the fullerene) while it does not dissolve the other (usually the polymer). It is in this way possible to favor the bicontinuous percolation pathways for exciton dissociation and charge transport through an additive-induced phase separation related to the additive boiling point and the degree of interaction between the additive and fullerene [97].

3.1.2. The use of additives

Apart from acting on the dissociating properties of donor/acceptor interfaces, as we will show, additives are also used for different purposes like increasing crystallinity, controlling the surface energy, improving miscibility or promoting vertical phase separation. Two basic requirements for the correct choice of an additive are: (a) The boiling point of the additive has to be much higher than the primary solvent, and (b) only one component will be selectively dissolved in the additive. For example, considering polymer:fullerene blends, only the fullerene is selectively dissolved in the selected additive [17]. Due to the higher boiling point of its preferred solvent, the fullerene will remain for longer in the liquid phase improving its crystallization and facilitating the integration of smaller fullerene domains into the polymer aggregates. This, results in a more favorable donor/acceptor interface density and domain size.

Some of the most studied additives are the ones based in alkanedithiols and 1,8-di(R)octanes.

3.1.2.1. Alkanedithiols. Due to the ability of alkanedithiols to selectively dissolve the fullerene component while the polymer is less soluble, an optimum nanomorphology is formed [17]. Peet et al. compared the performance of P3HT and PCPDTBT devices processed from pristine solvents and with blends of the same primary solvent and different alkanedithiols. In this way, reported improvements in the PCE from 2.8% to 5.5% when 1,8-octanedithiol (ODT) was added to chlorobenzene (CB) [53]. In a previous study, they also observed a larger photoresponsivity and increased hole mobility in P3HT:PCBM based devices when

using alkyl thiol molecules with respect to devices processed from pristine toluene [98]. It was observed that 5% of octanethiol increased the responsivity by a factor of 60, as well as the hole mobility in nearly two orders of magnitude. Coates et al. also demonstrated an enhanced photoconductivity response in PCPDTBT:PC₇₀BM based devices when using ODT as additive [99]. The increase primarily resulted from enhanced carrier mobility, and to a lesser extent, from a more efficient photogeneration of mobile carriers and longer mobile carrier lifetimes. The enhanced photoresponse is consistent with the increase in power conversion efficiency obtained from solar cells processed using ODT as additive.

3.1.2.2. 1,8-di(R)octanes. 1,8-di(R)octanes with different functional groups (R) are also often used as additives in order to favor the nanomorphology of the film that improves device efficiency. Fig. 5 represents the influence of 1,8-diiodooctane (DIO) in the final morphology of the film. When no additives are used, there are big aggregates of fullerene and the penetration of the acceptor molecules in the polymer network is more difficult, resulting in large fullerene and polymer domains. On the contrary, DIO is a much better solvent for the fullerene than CB while the polymer has limited solubility in DIO and it is very well solved in CB. With the addition of DIO in this case, the fullerene is selectively dissolved facilitating the percolation of acceptor molecules in the polymer network resulting in a more favorable nanomorphology of the film due to the optimization of the domain size and polymer:fullerene interface. Lou et al. indicated that the reason for the interaction between the fullerene and DIO and the consequent enhanced solubility of PC₇₀BM in presence of this additive, could be due to the fact that the iodine atom bears a partial negative charge while PC₇₀BM is electrodeficient [18].

The work carried out by Liang et al. for devices based on PTB7 show the influence of DIO in device performance when using it as additive [67]. Preliminary studies showed that PTB7:PC₇₀BM (1:1.5) films prepared from ODCB and DIO (97%:3% in volume) increased the fill factor from 60.25% to 68.9% and the PCE from 6.22% to 7.18%, in comparison to devices processed from pristine ODCB. In this case, the photocurrent remained constant. However, when chlorobenzene was used as the primary solvent, a considerable increment was observed also in the photocurrent (from 10.2 mA cm⁻² to 14.5 mA cm⁻²). Also the fill factor

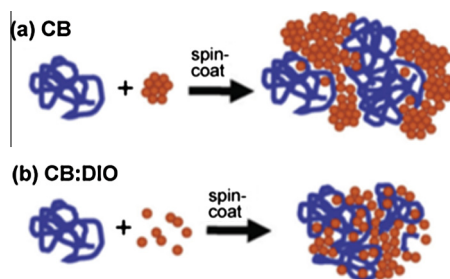


Fig. 5. Graphical sketch of polymer and fullerene when using only chlorobenzene as a solvent (a) and with diiodooctane (DIO) as an additive (b). Reprinted with permission from [18].

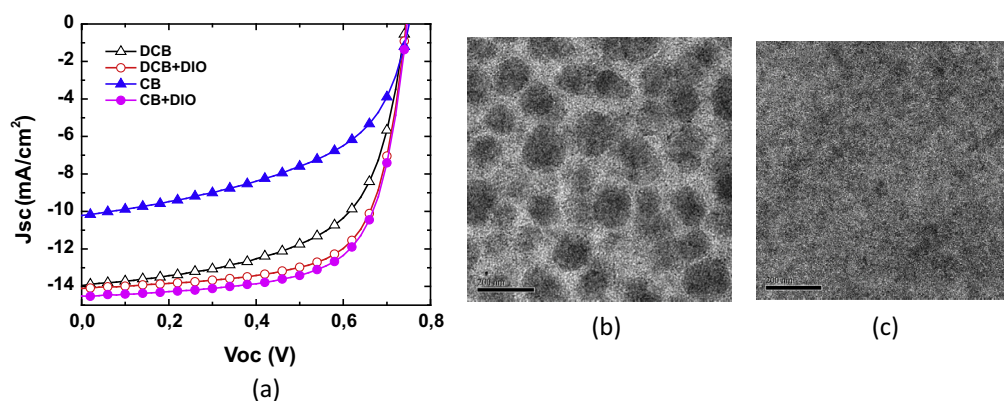


Fig. 6. (a) Current density–voltage curves of PTB7:PC₇₀BM devices using ODCB (open triangles), ODCB with 3% DIO (open circles), CB (filled triangles) and CB with 3% DIO (filled squares) as solvents. (b) and (c) are TEM images of PTB7:PC₇₀BM blend film prepared from CB without and with DIO, respectively. The scale bar is 200 nm. Reprinted with permission from [67] under license number 3538840445408.

Table 3

Device photovoltaic parameters of ODCB only, ODCB with 3% DIO, CB and CB with 3% DIO as solvent. Source [67].

	V_{oc} (V)	J_{sc} (mA cm ⁻²)	FF (%)	PCE (%)
DCB	0.74	13.95	60.25	6.22
DCB + DIO	0.74	14.09	68.85	7.18
CB	0.76	10.20	50.52	3.92
CB + DIO	0.74	14.50	68.97	7.40

rose from 50.52% to almost 69%. In this way, it was possible to improve the efficiency from 3.92% (when CB was used as solvent) up to 7.4% when DIO was used as an additive. All these data are collected in Fig. 6a and Table 3. They also studied the influence of the additive in the morphology of the active layer by Transmission Electron Microscopy (TEM). Images revealed that DIO promotes the formation of smaller domains. The film also showed a higher uniformity due to the good miscibility between PTB7 and PC₇₀BM and the formation of an interpenetrating network. In this way, higher FF and photocurrent values were achieved increasing thus the PCE.

Some other works have also shown the potential of DIO as an additive to improve the performance of devices made

from different active materials. Lee et al. demonstrated an enhancement from 3.4% up to 5.1% by using DIO in BHJ organic solar cells based on PCPDTBT:PC₇₀BM systems [16]. Zhang et al. reported a PCE increment from 1.4% to 4.8% when also DIO was used as the additive to process devices from a low bandgap polymer consisting in thieno-thiophene substituted benzodithiophene (PTTBDT-C8) [100]. Finally, Bijleveld et al. also documented the use of DIO for processing devices with DPPs [41]. They also observed an enhancement in the PCE from 2% to 5.6% and substantial changes in the film morphology when DIO was added to chloroform.

3.1.2.3. Alternative additives. Alternatively, some other approaches to afterwards manipulate the bulk morphology once the film has been already deposited from solution have been attempted with successful results. Zhou et al. spin coated methanol on top of an already dry active layer comprised by PTB7:PC₇₀BM [101]. They reported simultaneous improvements on device series resistance, charge mobility, charge recombination and charge extraction by mainly means of surface modification. The increased surface potential measured for methanol treated devices is

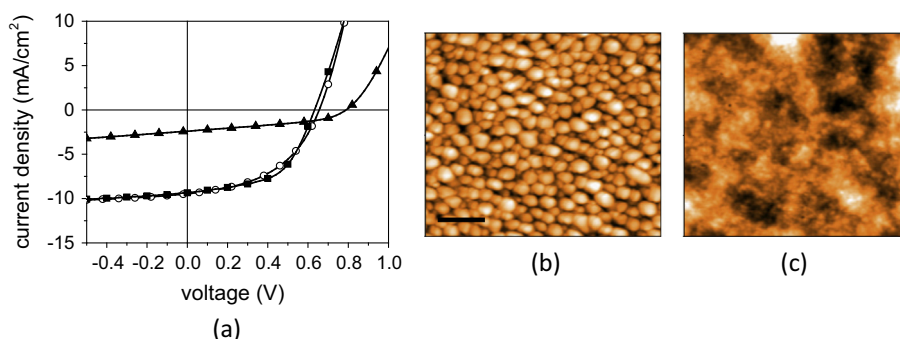


Fig. 7. (a) Current density–voltage measurements under AM 1.5G illumination (1000 W/m²) of pBBTDPP2:PC₆₀BM devices coated from different media: Chloroform (triangles), ODCB (open circles) and chloroform:ODCB mixture (squares). (b) Surface topography of a pBBTDPP2:PC₆₀BM film from chloroform. (c) Surface topography of a pBBTDPP2:PC₆₀BM film from chloroform:ODCB. Scale bar is 1 µm. Reprinted with permission from [56] under license number 3538970205811.

Table 4

Photovoltaic parameters of pBBTDPP2:PCBM solar cells. Source [56].

	J_{sc} (mA cm ⁻²)	FF	V_{oc} (V)	PCE (%)
pBBTDPP2:[60]PCBM from chloroform	2.4	0.41	0.78	1.1
pBBTDPP2:[60]PCBM from ODCB suspension	9.4	0.47	0.66	2.9
pBBTDPP2:[60]PCBM from chloroform:ODCB	9.4	0.54	0.63	3.2
pBBTDPP2:[70]PCBM from chloroform:ODCB	11.3	0.58	0.61	4.0

believed to be originated from the charge of surface electronic states including the diminishment of surface traps or variation of charge density. All these improvements gave rise to enhanced J_{sc} and FF that lead to 7.9% PCE devices in comparison to 7.1% for non-treated films.

3.1.3. Solvent mixtures

Similarly to additives, the combination of two or more solvents can help control the nanomorphology of the polymeric blend. Janssen et al. reported the influence of adding ODCB to chloroform in a series of DPP based devices performance [56,102]. The analysis was based in a narrow band-gap polymer known as pBBTDPP2, in combination with PC₆₀BM or PC₇₀BM diluted in chloroform (CHCl₃), ODCB or a mixture of both solvents. When the polymer:fullerene was dissolved in chloroform, just 1.1% of PCE was achieved. This low performance was attributed to the amorphous nature of the deposited layer. When using ODCB instead, due to the limited solubility of pBBTDPP2 in this solvent, after spin casting the solution, films with larger degrees of crystallinity were obtained, which resulted in devices with higher photocurrent values and thus higher PCEs, 2.9%. The PCE of pBBTDPP2 based devices was significantly improved by combining chloroform and ODCB. With the combination of these two solvents in a ratio of 4:1, a large degree of semi-crystalline polymer film was obtained. In this way, PCE values of 3.2% and 4% were achieved when using PC₆₀BM and PC₇₀BM as electron acceptors, respectively. Due to the large difference in vapor pressure, the final film morphology was essentially determined by the slow evaporation of ODCB, leaving the polymer sufficient time to partly crystallize before precipitation. Cells from chloroform:ODCB, apart from higher photocurrent values, provided also higher FFs with respect to the other two options (see Fig. 7a and Table 4). Atomic force microscopy (AFM) pictures revealed that chloroform:ODCB devices displayed only small features (<100 nm) while the chloroform ones contained domains with lateral dimensions of several hundreds of nm (see Fig. 7b and c).

Zhang et al. also observed a significant enhancement in the photocurrent density for a polyfluorene copolymer/fullerene blend. When introducing a small amount of chlorobenzene into the chloroform solvent, a uniform domain distribution was reached resulting in more efficient devices [103].

Chloronaphthalene (CN) is another secondary solvent widely used to act on internal bulk morphology. 1-CN in ODCB or small amounts of nitrobenzene in CB have also been used as binary solvent mixture for P3HT:PCBM based devices in order to also improve device performance with

the aim of achieving a higher degree of crystallinity [104,105]. Furthermore, CN has been used to promote a nanowire structure during the film-forming process [106]. Standard device efficiencies around 5.2% for a BDT-fluorinated benzothiadiazole copolymer derivative (PBTD2FBT) were improved to 8.2% with a simple binary solvent mixture. The enhanced photoconductivity of the nanowire-embedded photoactive layer increases photon harvesting and reveal a 60% improvement in overall efficiency with respect to devices without nanowires.

3.2. Bulk morphology control: The use of solubilizing side chains

The size and branching of solubilizing side chains in conjugated polymers is another important factor that affects the self-assembling properties and the bulk morphology in thin-film devices. This has been deeply studied for most of the copolymer families introduced in Section 2.1 with very promising results. Zhang et al. demonstrated that the dihedral angles between the BDT and conjugated side groups in PBDDTT based copolymers play an important role in the material crystallinity and aggregation size of the polymer [107]. Similarly, Cabanetos et al. demonstrated that replacing branched side chains by linear ones in the BDT moiety induces a critical change in the bulk morphology that results in a dramatic drop in device performance [108]. The latter is correlated with polymer self-assembly and backbone orientation. In contrast, they also show that for polymers with branched alkyl-substituted BDT units, controlling the number of aliphatic carbons in the linear N-alkyl-substituted TPD motifs can importantly improve material performance.

In a similar manner, Yiu et al. showed that linear side chains can be used to promote thin-film nanostructural order in a DPP derivative leading to a substantial increase in the efficiency of bulk heterojunction devices [109]. Li et al. also demonstrated the effect of the solubilizing alkyl side chain on the performance of DPP based devices [110,111]. The morphology of the blends is characterized by a semicrystalline fibrillar microstructure. The width of semicrystalline polymer fibrils is correlated with the EQE of the device. If the width of the fibril is wider than the exciton diffusion length, the efficiency drops. The fiber width is largely correlated with the solubility of the polymer that it is at the same time tuned with the length of side chains. Alternatively, moving the alkyl-chain branching position away from the polymer backbone also favorably modifies the thin-film morphology and improves the solar cell performance [65].

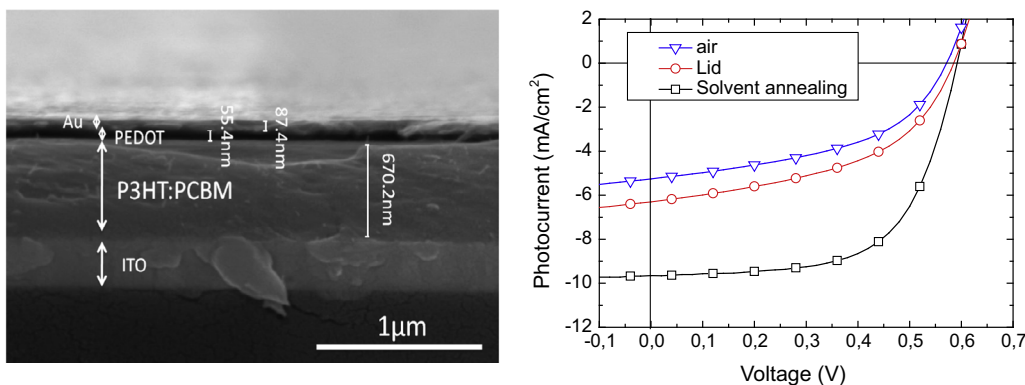


Fig. 8. (a) FESEM (Field emission scanning electron microscopy) cross sectional view of an inverted ITO/ZnO/P3HT:PCBM/PEDOT:PSS/Au solar cell. Different layers and their thickness are depicted. (b) J/V curves of different photoactive layer drying techniques.

Table 5

J/V characteristics of different photoactive layer drying techniques. Source [112].

Lid type	V_{oc} (V)	J_{sc} (mA cm ⁻²)	FF	PCE (%)
Dry in air	0.57	5.26	0.48	1.44
Lid	0.59	6.30	0.48	1.78
Lid + CB	0.59	9.65	0.62	3.57

3.3. Post-processing treatments

The possibility to act on film morphology while and after the deposition process, has also been thoughtfully studied. Firstly, it is possible to quite accurately control the drying time of the films by using alternative depositing techniques to spin coating as for example Dr. Blading. Based in the work carried out by Li et al. about the slow drying for film nanomorphology control in conventional architecture devices [11], we also slowed down the drying process of the P3HT:PCBM photoactive film in inverted configuration devices (600 nm thick photoactive layer, see Fig. 8a) [112]. Film drying times were delayed from 1–2 s to ≈ 10 s and ≈ 30 s for films dried directly in air, protecting the film with a petri dish as a lid in order to limit the contact of the film with air and creating a solvent atmosphere below the petri plate to minimize the presence of air, respectively. After the different film drying procedures a common annealing step at 140 °C for 15 min was always necessary in order to crystallize the P3HT.

Results revealed that the slow drying of the film assists the growth of a photoactive self-ordered nanostructure improving the PCE from 1.44% to 3.57% (see Fig. 8b and Table 5). The self organization of the polymer has been shown to improve field effect carrier mobilities by more than a factor of 100 in P3HT [113,114]. On the contrary, the destruction of self-organized structures during fast drying (unordered growth) present unbalanced charge carriers and lower charge mobilities [11]. Under these precisely controlled drying conditions it is feasible to increase the thickness of the active film up to 600 nm, maximizing thus the light absorption without affecting charge transport negatively. Raising the Dr. Blade plate temperature from ambient conditions to 70 °C had a similar effect.

Finally, a novel approach explores the viability of vapor printing as a fast post-processing technique [115,116]. A carrier gas transporting vapor solvent is delivered through a nozzle promoting local self-assembly of polymer chains. This enables finding an optimal nanostructure in promisingly short times. Changes in the degree of crystallinity led to a twofold increase in PCE with respect to as-cast samples.

4. Device layout/architectures

All the layers that form an organic solar cell have a direct influence in the performance of the device. Buffer interlayers are of crucial interest in order to increase the efficiency of devices. The use of interfacial materials dates back from the very beginning of the OLED development when PEDOT:PSS, calcium (Ca), and LiF were initially used with the objective of modifying and improving the charge injection properties from the purely metallic electrodes to the emitting semiconductor [117–119]. The working principles behind these –sometimes insulating materials– are not yet totally understood. Some of them are used to smoothen the rough profile of underlying films and avoid shunts. Others are used to modify the work function of the metal and align it to some extent with the HOMO and LUMO levels of the semiconductor favoring thus an ohmic contact. Last but not least, ionic compounds are believed to form interfacial dipoles that help charge injection/extraction and at the same time generate optimal optical interferences that improve the light harvesting of devices [69,120].

The device architecture can also alter the efficiency of an organic cell. In some cases, inverting the polarity of the cell can also have a positive influence in device performance due to vertical segregation of the mixed compounds that generate a more favorable donor and acceptor material concentration gradient leading to a more efficient charge transport process through the film [121,122].

Moreover, the processing of more complicated architectures such as tandem cells that comprise two connected cells made of polymers with complementary absorption spectra can also result in high efficiency devices due to enhanced light absorption [19].

All these device layout/architecture aspects that have a direct influence in the PCE of devices but are not strictly related to either absorbers intrinsic properties or nano-morphology of the film will be addressed in this section.

4.1. Alternative interlayers

An efficient charge extraction process following light absorption and charge generation requires the use of conducting electrodes wisely chosen in order to have energetic levels alignment and hence ideally ohmic contacts between the metal and the semiconductor and avoid thus charge barriers and undesired losses. Depositing an extra buffer layer between the photoactive film and the metallic electrode, has been demonstrated as an efficient way to improve the contact properties and selectivity, to enhance the charge extraction from the active film to the electrode and to maximize the light harvesting via constructive interferences between the incident and reflected light.

Indium tin oxide (ITO) is typically used as the bottom contact (anode) in conventional configuration organic solar cells. ITO has a high work function around 4.8 eV that it is very dependent on washing treatments [118,123]. However, these variations and the roughness of the resulting films usually results in important contact losses [124]. In order to improve the quality of this contact and favor the formation of an ohmic contact, a p-type PEDOT:PSS interlayer which has a work function of 5 eV has been traditionally used [125]. Due to the acidic nature of PEDOT:PSS and its tendency to be easily degraded in contact with either air or moisture and negatively affect the stability of the whole device, different transition metal oxides such as V_2O_5 , MoO_3 , WO_3 and NiO , that are considered more stable, were introduced as alternative p-type interlayers in relatively high efficient and stable devices [38,126,127].

In the cathode side instead, calcium was initially inherited from the OLED development as the hole blocking layer due to its low work function. In spite of the good results obtained also for photovoltaic devices in combination with silver, it is however also very reactive to oxygen and moisture and thus device stability is further jeopardized. Alternative inorganic low work function interlayers were introduced. In one side, inorganic salts as LiF [128–130],

CsF [131,132], MgF [133] have been vacuum evaporated in combination with aluminum in order to enhance the contact selectivity and hence the PCE. It is believed that due to their high internal dipole moment, thin layers of these materials are able to alter the electrode work function by inducing a shift of the vacuum energy level. Regardless of the increase in efficiency obtained with the use of these materials, they are principally vacuum deposited which hinders the way toward lower cost devices based of R2R processing. Moreover, these metal salts are also prone to degradation in contact with air. In order to avoid this fast degradation and improve stability of devices, solution processable films of n-type inorganic semiconductors as TiO_x and ZnO processed from nanoparticle dispersions are typically used as n-type interlayers [30,134–136]. Solution processable alternatives make use of salts like ZnS [137], LiAc [138] or Cs_2CO_3 [139–141]. Furthermore, polymeric salt compounds, known as polyelectrolytes have been used with promising results [142]. Also small molecules with opposing internal charges, zwitterions, have been demonstrated as interfacial layers in organic solar cells [143,144]. Khan et al. demonstrated efficient conventional configuration P3HT:ICBA base solar cells substituting the Ca layer by a thin film of a hydrophilic polymer processed from a polyethylenimine, 80% ethoxylated solution, PEIE [145]. As a result devices with V_{oc} of 0.78 V, J_{sc} of 9.1 mA cm^{-2} , FF of 65% and PCE of 4.6% were achieved. Soluble fullerene derivatives have been also successfully demonstrated as a potential interfacial layer material to replace LiF [146,147].

Nowadays, many research groups, mainly motivated by the improvement observed in the FF and the parallel resistance, have focused their investigation in alternative interlayers that can further enhance the device overall performance. As it was shown in a previous section, Liang et al. improved the PCE of ITO/PEDOT:PSS/PTB7:PC₇₀BM/Ca/Al based organic solar cells from 3.92% to 7.40% by adding 3% of DIO to the primary solvent CB [67]. However, more specifically related to the use of effective interlayers, further improvement was carried out by He et al. when a thin polymeric film of PFN was incorporated as the cathode interlayer, increasing the PCE to 8.37%. Significant and simultaneous enhancements in J_{sc} , V_{oc} , FF were observed

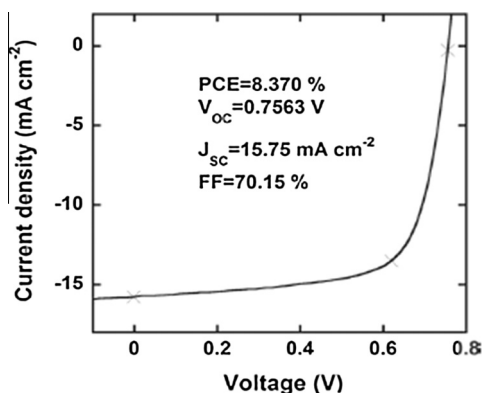


Fig. 9. Current–voltage characteristics of PTB7:PC₇₀BM based solar cells using PFN as the cathode interlayer. Reprinted with permission from [68] under license number 3538970497548.

(see Fig. 9) [68]. PFN is an alcohol/water soluble conjugated polymer that creates an interfacial dipole between the PFN and the polymeric PTB7:PC₇₀BM blend. Moreover, the incorporation of PFN is believed to exert a strong electric field at the active layer/cathode interface that may strongly influence charge transport and extraction [148]. Thus, the effects of the interlayer on the improvement of device performance were due to improved charge-transport properties, reduction of any possible space charge effect at the interface and reduced surface recombination losses [149]. Following this approach, a growing number of water/alcohol-soluble conjugated polymers and small molecules are being synthesized. They can be processed from water or other polar solvents and allow the fabrication of multilayer organic devices without interface mixing by solution processing. Thanks to promising interface modification ability, they can greatly increase the efficiency of solar cell devices [150,151]. Regarding dipole formation at this interface and related to morphology issues -previously addressed in the last section-, it has been also recently suggested that vertical segregation of the fullerene content toward the cathode can also result in interfacial dipoles of varying strength that affect the selectivity of the contact in a similar way as buffer interlayers [152,153].

Alternatively, Martínez-Otero et al. incorporated bathocuproine (BCP) as the interlayer of the cathode to achieve an optimal optical interference for PBDTTT-C and PTB7 based devices. As a result, for devices processed with BCP as interlayer instead of Ca, an increment in PCE from 6.3% to 7.5% was observed for PBDTTT-C based cells and from 7.4% to 8.1% for the PTB7 based ones [120]. In the case of PTB7 the increment in PCE was related to the increase in photocurrent due to the enhanced reflectivity of the buffer layer/electrode back contact. For the PBDTTT-C instead, apart from the photocurrent improvement, the FF was also enhanced from 60.3% to 67.9%, which was related to the reduction of recombination at the interfaces.

4.2. Inverted configuration

As previously commented at the beginning of the section, inverting the polarity of the device and processing thus the electron collecting electrode onto the ITO and the hole collection electrode on top of the active layer has also been successfully used to increase the efficiency of devices made with the same active materials. Ajuria et al. documented this effect to P3HT:PCBM devices for which impressive FFs over 70% were reported for inverted designs [154].

In the case of PTB7 devices, further improvement in PCE was observed by He et al. when inverting the polarity of the device, reaching a very remarkable 9.2% [69]. As it can be seen in Fig. 10 and Table 6 the efficiency improvement for inverted structure devices is mainly due to the larger J_{sc} with respect to the conventional one, 17.2 mA cm⁻² in comparison to 15.4 mA cm⁻², respectively. The drastically enhanced J_{sc} for inverted devices was assigned to an improved ohmic contact that eases photogenerated charge carrier collection and an optimum photon harvesting of these devices.

The interlayers used for inverted configurations can also be exposed to different treatments in order to modify their intrinsic properties and try to improve device efficiency. Adhikary et al., improved PBDTTT-CT:PC₇₀BM based inverted configuration devices from 6.46% to 8.34% by exposing the cell to UV-ozone [72]. This treatment modifies the wurtzite phase crystallinity of the ZnO films leading to faster film mobilities and improved charge extraction properties. While exposure times around 5 min resulted in an ideal crystalline structure longer exposure times induced the formation of p-type defects pushing the ZnO Fermi-level further away from the vacuum level, and decreasing the wurtzite crystallinity.

The work function of the materials can be also manipulated by surface modifiers. Zhou et al. demonstrated that

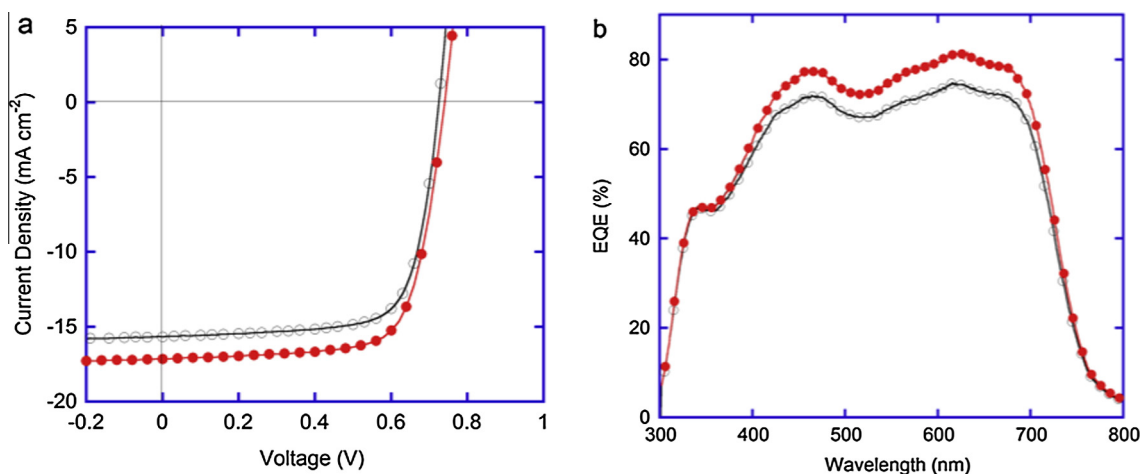


Fig. 10. Performance for inverted configuration (red filled symbols) (ITO/PFN/PTB7:PC₇₀BM/MoO₃/Al) and conventional configuration (black open symbols) (ITO/PEDOT:PSS/PTB7:PC₇₀BM/PFN/Ca) devices. (a) Current density–voltage measurements and (b) EQE graph. Reprinted with permission from [69] under license number 3538860411703. (For interpretation of the references to color in this figure legend, the reader is referred to the web version of this article.)

Table 6

Best device performance/parameters for PTB7:PC₇₀BM based conventional and inverted solar cells with PFN as interlayer. Source [69].

Device type	PCE (%)	J_{sc} (mA cm ⁻²)	FF (%)	V_{oc} (V)
Conventional	8.24	15.4	70.6	0.759
Inverted	9.15	17.2	72.0	0.740
Inverted, tested by CPVT	9.214	17.46	69.99	0.754

compounds based on polymers containing simple aliphatic amine groups can substantially reduce the work function of conductors including metals, transparent conductive metal oxides, conducting polymers, and graphene [155]. Kyaw et al. incorporated polyethylenimine, 80% ethoxylated (PEIE) on top of ZnO to enhance the efficiency of the cell by lowering the work function of ZnO (from 4.5 eV to 3.8 eV) [156]. With this surface modification, the PCE was enhanced from 6.29% to 7.88% for inverted configuration p-DTS(FBTTh₂)₂:PC₇₀BM based small molecule solar cells thanks to simultaneous enhancements in J_{sc} , V_{oc} and FF.

4.3. Tandem cells

The main losses that occur in a solar cell are transmission and thermalization losses (see Fig. 11a). Photons with lower energy than the energy bandgap will not be able to generate excited states resulting therefore in transmission losses. On the contrary, photons with energies larger than the energy bandgap will generate hot charge carriers that will relax down to the LUMO of the polymer, giving rise to thermalization losses [7,157–160]. By stacking together in the same device two cells with polymers that absorb at different wavelengths, i.e. wide and low bandgap polymers, these losses can be reduced. On the one hand, the reduction in thermalization losses can be carried out by conversion in the subcell with a wide bandgap polymer. On the other hand, transmission losses are lowered by absorption of the low energy photons in the subcell with a low bandgap polymer. This results in polymer solar cells with ideally enhanced power conversion efficiencies.

Tandem solar cells basically consist on stacking two or more devices one on top of each other with an adequate interlayer between them (see Fig. 11b). The first deposited

subcell is usually referred as the front cell while the one that is deposited on top is referred as the back cell. The connection among the subcells can be performed either in series (two terminals) or in parallel (three terminals) [159,161,162].

Shockley and Queisser showed that under 1 Sun irradiance, the maximum power conversion efficiency of a single p–n junction solar cell taking into account thermodynamic considerations is 30% [157]. According to the De Vos, this limit can be risen to 42% when stacking two subcells in a tandem with energy gaps of 1.9 and 1.0 eV. Finally, if three subcells with complementary energy gaps of 2.3, 1.4 and 0.8 eV are implemented into a tandem, the conversion limit rises to 49% [158,163].

Simple models have been also developed for organic tandem devices in order to predict the efficiency increase when going from single to tandem cells. These models are based in the energy bandgaps of the absorbers used in each subcell and efficiencies up to 15% were initially estimated with the appropriate combination of materials [164,165]. Nowadays, recent more accurate models predict maximum efficiencies over 20% for this configuration [3].

The absorption spectra of these polymers usually show narrow peaks restricting the absorbance of the cell to a small part of the solar spectrum. Therefore, materials with complementary absorptions are stacked together in the same tandem device in order to broaden the overall absorption of the resulting cell and cover more efficiently the emission spectrum of the Sun [19,20,158,159,166–174]. Moreover, single cells have usually their efficiency compromised between light absorption and charge transport. Even though, polymers show relatively large absorption coefficients, especially at their maxima, thick films are used in order to harvest as much light as possible also at the onset of the absorption. This is an issue for low carrier mobility and lifetime polymers that negatively affect the FF. Thick photoactive layers can be often avoided in the tandem configuration with the objective of increasing the light absorption and output current [158,159,161,175]. Its use can be limited to cases when the back cell provides a much larger photocurrent than the front one [176]. Thus, the front layer should ideally only absorb most of the light corresponding to wavelengths of its

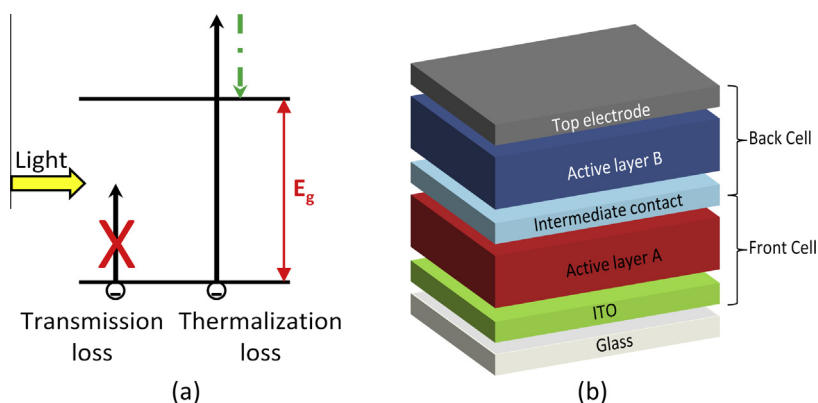


Fig. 11. (a) Thermodynamic losses related to light absorption. (b) Layout of an organic tandem cell with two devices stacked one on top of each other.

maximum absorption coefficient. On the contrary, the light that is not absorbed by the front cell belonging to wavelengths of maximum absorption of the second layer will be more efficiently absorbed by the polymer of the back cell. Thus the solar irradiance is absorbed in a more efficient manner without the need of thick layers that can induce charge transport losses.

One of the first reports about organic tandem solar cells with two identical small molecule subcells stacked together separated by a thin gold (Au) layer was published in 1990 by Hiramoto et al. [177]. As the processing of small molecule tandem cells is a dry process, several subcells can be stacked one on top of each other without many problems. However, due to the limited choice of small molecule materials with significantly different absorption spectra, they started exploring hybrid tandem cells combining polymer and small molecule subcells [169,178–181]. In 2005, Kawano et al. reported the first tandem cells composed of two identical polymer bulk heterojunction subcells stacked together with an interlayer comprised by sputtered ITO and spin coated PEDOT:PSS [182]. One year later, Hadipour et al. showed a tandem cell consisting of subcells based on low and wide bandgap polymers with complementary absorptions [170]. However all these attempts resulted in efficiencies below 5% and many times even below those efficiencies reported for single cells made with one of the same comprising materials. A major breakthrough in the area of polymeric tandem cells was the demonstration of all solution processable polymer tandem cells with efficiency over 6% by Kim et al. [167]. More recently, in 2010 Gilot et al. studied

the effect of current matching on the tandem device performance which provides more insight in order to achieve high performance tandem cells [174]. It is worth saying that the performance of polymeric tandem cells during the last 4 years has been limited to around 7% mainly due to the lack of high performing low bandgap polymers [171,172,174,183]. Nevertheless, in 2012 Dou et al. designed a new low bandgap polymer and achieved an inverted configuration tandem device with 8.6% PCE [173,184]. Later, Kim et al. also reported a 8.6% efficient tandem cell comprising a P3HT bottom cell and a new synthesized low bandgap co-polymer alternating thienothiophene substituted BDT (TTBDT) and fluorothiophene-carboxylate (FTT) as the front cell [185]. Recently, Li et al. demonstrated tandem and triple junction polymer solar cells with power conversion efficiencies of 8.9% and 9.6%, respectively, by combining a low bandgap polymer known as PMDPP3T (with absorption in the near-infrared region up to 960 nm) and the wide bandgap polymer PCDTBT [20].

Single cells based on PMDPP3T:PC₆₀BM and PCDTBT:PC₇₀BM result in devices of 6% and 4.7% PCE, respectively. However, using the same layer thicknesses and stacking the subcells in a tandem cell (see Fig. 12a), the PCE was enhanced to 8.9%. Further improvement in the efficiency of the organic solar cell was carried out by adding an additional layer of the same small bandgap material creating a triple junction device, as the one depicted in Fig. 12d. In a tandem cell the J_{sc} is limited by the wide bangap front cell. However, this limitation is circumvented by splitting the small bandgap subcell into two separate cells

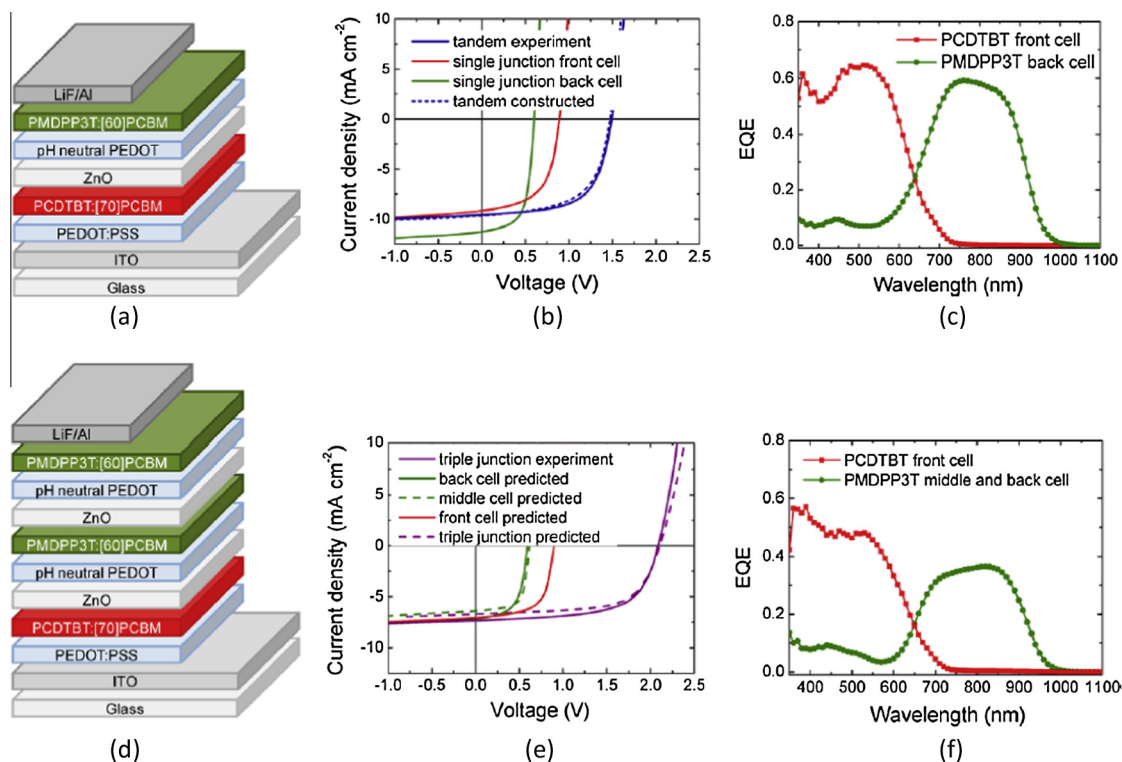


Fig. 12. Tandem and triple junction device layout (a, d), JV-characteristics (b, e) and EQE graph (c, f). Reprinted with permission from [20].

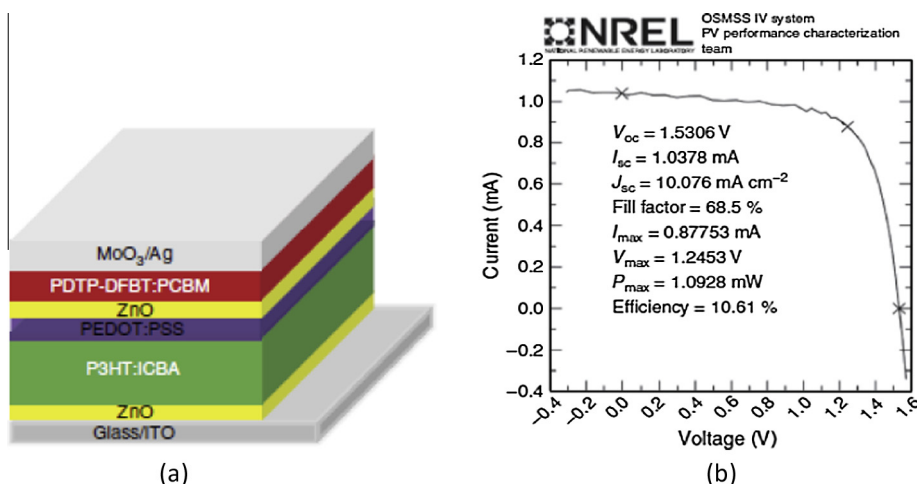


Fig. 13. (a) Device structure of the tandem solar cell and (b) J/V characteristics of the tandem cell as measured by NREL. Reprinted with permission from [19] under license number 3538861144913.

(middle and back cell) with different thicknesses to ensure that both absorb the same number of photons. The increased in V_{oc} of the triple junction (2.09 V with respect to 1.49 V) compensates the loss in J_{sc} (compare Fig. 12b and c with Fig. 12e and f). In this way, the efficiency was enhanced up to 9.6% [20].

Efficiencies up to 10.2% have been also published by You et al. stacking together in a tandem device two identical subcells based on PDTP-DFBT:PC₇₀BM [186]. It is worth mentioning that single PDTP-DFBT:PC₇₀BM based devices provide efficiencies of 8.1%. Thin films of 80 nm yield smaller photocurrents than thicker films of 120 nm (17 mA cm⁻² and 19 mA cm⁻² respectively), but show improved charge transport properties according to the measured FFs (65% and 58%). This points to charge transport issues that penalize the performance of thick films, and suggests that the performance of single cells for this material is a difficult compromise between light absorption and charge transport. When implemented in tandem configuration, the lack of absorption of thinner films can be compensated by the extra absorption of the second cell that additionally offers a gain in V_{oc} . In this way, the absorption in the visible part of the tandem cell with both thin layers was significantly increased from 70% to 90% with respect to that of the single cell, maintaining the FF around 65%.

The best polymer–fullerene tandem solar cells have a reported certified efficiency of 10.6% (see Fig. 13b) and feature a response up to 900 nm [19]. A wide bandgap polymer, P3HT, was blended with ICBA in the front cell. As commented previously, this combination allows for a

larger obtained V_{oc} in comparison to more standard fullerene derivatives. The low bandgap polymer PDTP-DFBT was used with either PC₆₀BM or PC₇₀BM as the back cell (see Fig. 13a). In Table 7, the detailed parameters of single and tandem cells are summarized. As it can be seen, single cells provide efficiencies of 6.1% and 7.1% for P3HT:ICBA and PDTP-DFBT:PC₆₀BM, respectively. The photocurrent of the tandem is obviously limited by the subcell with the lowest value. This is clearly the case for the tandem that makes use of PC₆₀BM in the back cell, whose photocurrent is very similar to that measured for an equivalent single cell of the front cell. However, when PC₇₀BM is used the current of both cells are unbalanced and penalizes the overall performance of the tandem with additional losses that result in a photocurrent even lower than that of the limiting subcell. The V_{oc} is the perfect summation of each subcell, resulting in this way in the most efficient reported tandem device to date (see Table 8).

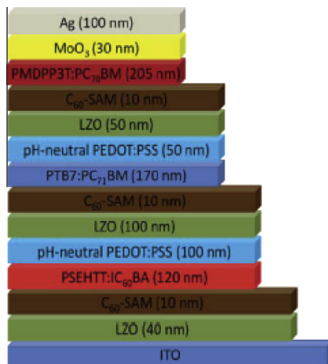
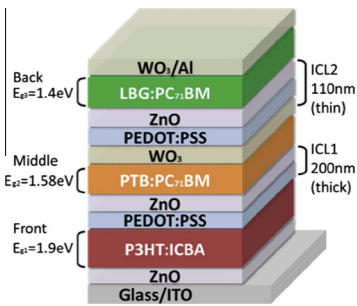
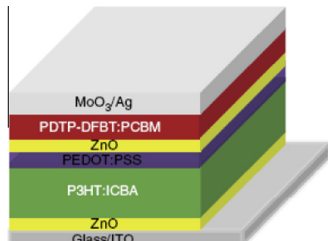
Even though as commented before, triple-junction devices can in some cases minimally improve the performance of tandem cells [20], they are very difficult and costly to implement. The enhancement obtained in terms of efficiency does not always compensate these two issues and one has to carefully analyze whether this approach is worthy taking into account a potential mass production. In any case, and considering only efficiency issues, an efficient triple-junction tandem organic solar cell with a record conversion efficiency of 11.5% has been recently published [187]. Three complementary absorbers with bandgap energies from 1.4 to 1.9 eV are used to obtain balanced

Table 7
P3HT and PDTP-DFBT single junction cell and tandem solar cell performance. Source [19].

Devices	V_{oc} (V)	J_{sc} (mA cm ⁻²)	FF (%)	PCE (%)
P3HT:ICBA	0.84	10.3	71.1	6.1
PDTP-DFBT:PC ₆₁ BM	0.70	15.4	66.2	7.1
PDTP-DFBT:PC ₇₁ BM	0.68	17.8	65.0	7.9
P3HT:ICBA/PDTP-DFBT:PC ₆₁ BM (Tandem 1)	1.53	10.1	68.5	10.6
P3HT:ICBA/PDTP-DFBT:PC ₇₁ BM (Tandem 2)	1.51	9.8	69.2	10.2

Table 8

List of most efficient polymer solar cells published to date.

N junction	Active materials	PV performance	[Ref]	Cell structure
Triple junction	PSEHTT:IC ₆₀ BA	PCE = 11.83%	[188]	
	PTB7:PC ₇₁ BM PMDPP3T:PC ₇₀ BM	FF = 0.67 $J_{sc} = 7.83 \text{ mA cm}^{-2}$ $V_{oc} = 2.24 \text{ V}$		
	P3HT:ICBA	PCE = 11.55%	[187]	
	PTB7-Th:PC ₇₁ BM PDTP-DFBT:PC ₇₁ BM	FF = 0.66 $J_{sc} = 7.63 \text{ mA cm}^{-2}$ $V_{oc} = 2.28 \text{ V}$		
Double junction	P3HT:ICBA	PCE = 10.6%	[19]	
	PDTP-DFBT:PC ₆₁ BM	FF = 0.68 $J_{sc} = 10.1 \text{ mA cm}^{-2}$ $V_{oc} = 1.53 \text{ V}$		

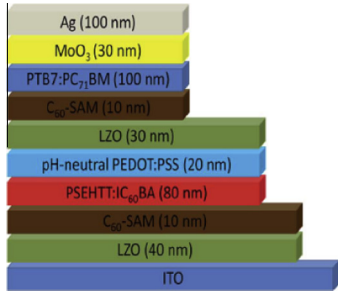
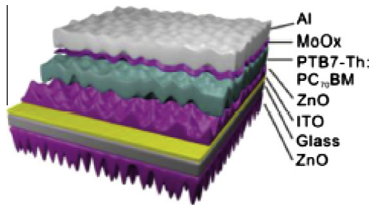
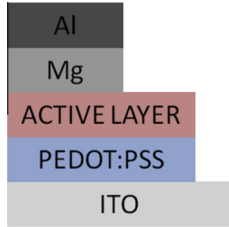
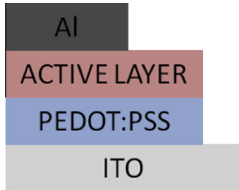
Reprinted with permission from [188] under license number 3538931411480. Copyright 2014 Royal Society of Chemistry

Reprinted with permission from [187] under license number 3538960907359. Copyright 2014 John Wiley and Sons

Reprinted with permission from [19] under license number 3538861144913. Copyright 2013 Nature Publishing group

(continued on next page)

Table 8 (continued)

N junction	Active materials	PV performance	[Ref]	Cell structure
	PSEHTT:IC ₆₀ BA PTB7:PC ₇₁ BM	PCE = 10.4% FF = 0.65 J_{sc} = 10.30 mA cm ⁻² V_{oc} = 1.54 V	[188]	
Single junction	PTB7-Th:PC ₇₀ BM	PCE = 10.1% FF = 0.70 J_{sc} = 19.47 mA cm ⁻² V_{oc} = 0.77 V	[70]	<p>Reprinted with permission from [188] under license number 3538931411480. Copyright 2014 Royal Society of Chemistry</p> 
	PBDT-TS1:PC ₇₁ BM	PCE = 9.5% FF = 0.68 J_{sc} = 17.46 mA cm ⁻² V_{oc} = 0.80 V	[45]	<p>Reprinted with permission from [70] under license number 3540360812490. Copyright 2014 John Wiley and Sons</p> 
	PPDT2FBT:PC ₇₀ BM	PCE = 9.4% FF = 0.73 J_{sc} = 16.30 mA cm ⁻² V_{oc} = 0.79 V	[40]	

absorption rates and matched photocurrents among the three subcells. In similar terms, Yusoff et al. made use of a combination of a wide bandgap, a medium bandgap and a low bandgap materials to report double junction devices of 10.4% and a record efficiency of 11.83% for a triple-junction cell [188] (see Table 8). The wide bandgap material was a copolymer based on the alternation of dithienosilole, thiophene and thiazolothiazole segments (PSEHTT) whose bandgap lies at 1.82 eV, while the medium and low bandgap materials were the already introduced PTB7 (1.6 eV) and PMDPP3T (1.3 eV) respectively. Apart from the active materials, this work also makes use of all the other concepts mentioned in the other sections of this review introducing for example new interlayers based on lithium zinc oxide and C60-self assembled monolayers. The resulting devices show impressive J_{sc} of 10.30 and 7.83 mA cm⁻², FF of 65.5 and 67.5 and V_{oc} of 1.54 and 2.24 V for the tandem (PSEHTT:ICBA//PTB7:PC70BM) and triple device (PSEHTT:ICBA//PTB7:PC70BM//PMDPP3T:PC70BM) respectively.

5. Summary

In this letter, we have initially presented the fundamental limits of polymeric solar cells, the factors that limit their performance and the different possible approaches to maximize it. We have then offered a comprehensive and detailed review of the most efficient attempts to overcome the long ambitioned 10% PCE in polymeric devices. We have divided the development of polymeric solar cells in three categories indicating the most efficient attempt for every case (Table 8):

– Materials:

- 10% PCE devices have been reported for a benzodithiophene device (PTB7-Th) incorporating deterministic aperiodic nanostructures (DANs) for broad angle light manipulation.
- 9% PCE devices have been reported for benzodithiophene and dithienopyran-difluorobenzothiadiazole derivatives as PTB7, PBDT-TS1 and PPDT2FBT.
- 8% PCE devices have been published for:
 - A fluorinated benzothiadiazole unit conjugated to a dithienopyran segment (PDTP-DFBT)
 - Conjugations of the diketopyrrolopyrrole moiety to thiophene-phenylene-thiophene segments in combination to a terthiophene unit (PDPP3TaltTPT)
 - A fluorinated benzothiadiazole unit conjugated to a benzodithiophene unit (PBDT2FBT)
- 7% PCE devices are already routinely achieved with the use of multiple diketopyrrolopyrrole and indenodithiophene derivatives
- Traditional fullerene derivatives such as PC₆₀BM and PC₇₀BM are still used in all the most efficient reported devices
- Alternative non-fullerene acceptors such as naphthalene diimide and triimide derivatives are starting to produce competitive efficiencies

– Strategies (fabrication/processing procedures): With the use of additives, solvent mixtures and post-

processing treatments it is possible to obtain an accurate control of the bulk morphology that results in improved efficiencies for a large variety of different polymer families.

– Device layout/architectures:

- Alternative interlayers of polymeric films and/or inorganic semiconducting oxides have considerably improved the PCE of devices reaching 9% for the most efficient donors.
- Inverted configuration has been also demonstrated as an efficiency improvement for different polymeric donors, in particular for benzodithiophenes as PTB7 and PBDTTT with overall efficiencies over 9% and 8% respectively.
- Tandem cells are the best approach to maximize light harvesting and device efficiency. The record reported polymeric device yields 10.6% and makes use of a single polythiophene as P3HT as the wide band gap absorber and a fluorinated benzothiadiazole derivative (PDTP-DFBT) as the low band gap absorber. Three complementary absorbers implemented in a triple junction solar cell have taken the record efficiency of organic solar cells to 11.83%.

Acknowledgements

We thank the European Community's Seventh Framework Programme (FP72007–2013) under Grants Nos. 287818 and 604397 of the X10D and ARTESUN projects respectively for providing financial support.

References

- [1] J. Nelson, *The Physics of Solar Cells*, Imperial College Press, 2003.
- [2] M.C. Scharber, N.S. Sariciftci, Efficiency of bulk-heterojunction organic solar cells, *Prog. Polym. Sci.* 38 (2013) 1929–1940.
- [3] N. Li, D. Baran, G.D. Spyropoulos, H. Zhang, S. Berny, M. Turbiez, T. Ameri, F.C. Krebs, C.J. Brabec, Environmentally printing efficient organic tandem solar cells with high fill factors: a guideline towards 20% power conversion efficiency, *Adv. Energy Mater.* 4 (2014). n/a–n/a.
- [4] C.J. Brabec, A. Cravino, D. Meissner, N.S. Sariciftci, T. Fromherz, M.T. Rispens, L. Sanchez, J.C. Hummelen, Origin of the open circuit voltage of plastic solar cells, *Adv. Funct. Mater.* 11 (2001) 374–380.
- [5] M. Lenes, G.-J.A.H. Wetzelaer, F.B. Kooistra, S.C. Veenstra, J.C. Hummelen, P.W.M. Blom, Fullerene bisadducts for enhanced open-circuit voltages and efficiencies in polymer solar cells, *Adv. Mater.* 20 (2008) 2116–2119.
- [6] F.B. Kooistra, J. Knol, F. Kastenberg, L.M. Popescu, W.J.H. Verhees, J.M. Kroon, J.C. Hummelen, Increasing the open circuit voltage of bulk-heterojunction solar cells by raising the LUMO level of the acceptor, *Org. Lett.* 9 (2007) 551–554.
- [7] G. Dennler, M.C. Scharber, C.J. Brabec, Polymer–fullerene bulk-heterojunction solar cells, *Adv. Mater.* 21 (2009) 1323–1338.
- [8] J.K.J. van Duren, A. Dhanabalan, P.A. van Hal, R.A.J. Janssen, Low-bandgap polymer photovoltaic cells, *Synth. Met.* 121 (2001) 1587–1588.
- [9] A. Dhanabalan, J.K.J. van Duren, P.A. van Hal, J.L.J. van Dongen, R.A.J. Janssen, Synthesis and characterization of a low bandgap conjugated polymer for bulk heterojunction photovoltaic cells, *Adv. Funct. Mater.* 11 (2001) 255–262.
- [10] T. Stübinger, W. Brütting, Exciton diffusion and optical interference in organic donor–acceptor photovoltaic cells, *J. Appl. Phys.* 90 (2001) 3632–3641.
- [11] G. Li, V. Shrotriya, J. Huang, Y. Yao, T. Moriarty, K. Emery, Y. Yang, High-efficiency solution processable polymer photovoltaic cells by self-organization of polymer blends, *Nat. Mater.* 4 (2005) 864–868.

- [12] W. Ma, C. Yang, X. Gong, K. Lee, A.J. Heeger, Thermally stable, efficient polymer solar cells with nanoscale control of the interpenetrating network morphology, *Adv. Funct. Mater.* 15 (2005) 1617–1622.
- [13] H. Hoppe, N.S. Sariciftci, Morphology of polymer/fullerene bulk heterojunction solar cells, *J. Mater. Chem.* 16 (2006) 45–61.
- [14] S. Sam-Shajing, Z. Cheng, L. Abram, C. Soobum, S. Kang, Carl E. Bonner Jr., D. Martin, S. Niyazi Serdar, Photovoltaic enhancement of organic solar cells by a bridged donor–acceptor block copolymer approach, *Appl. Phys. Lett.* 90 (2007) 043117.
- [15] S. Miller, G. Fanchini, Y.-Y. Lin, C. Li, C.-W. Chen, W.-F. Su, M. Chhowalla, Investigation of nanoscale morphological changes in organic photovoltaics during solvent vapor annealing, *J. Mater. Chem.* 18 (2008) 306–312.
- [16] J.K. Lee, W.L. Ma, C.J. Brabec, J. Yuen, J.S. Moon, J.Y. Kim, K. Lee, G.C. Bazan, A.J. Heeger, Processing additives for improved efficiency from bulk heterojunction solar cells, *J. Am. Chem. Soc.* 130 (2008) 3619–3623.
- [17] A. Pivrikas, H. Neugebauer, N.S. Sariciftci, Influence of processing additives to nano-morphology and efficiency of bulk-heterojunction solar cells: a comparative review, *Sol. Energy* 85 (2010) 1226–1237.
- [18] S.J. Lou, J.M. Szarko, T. Xu, L. Yu, T.J. Marks, L.X. Chen, Effects of additives on the morphology of solution phase aggregates formed by active layer components of high-efficiency organic solar cells, *J. Am. Chem. Soc.* 133 (2011) 20661–20663.
- [19] J. You, L. Dou, K. Yoshimura, T. Kato, K. Ohya, T. Moriarty, K. Emery, C.-C. Chen, J. Gao, G. Li, Y. Yang, A polymer tandem solar cell with 10.6% power conversion efficiency, *Nat. Commun.* 4 (2013) 1446.
- [20] W. Li, A. Furlan, K.H. Hendriks, M.M. Wienk, R.A.J. Janssen, Efficient tandem and triple-junction polymer solar cells, *J. Am. Chem. Soc.* 135 (2013) 5529–5532.
- [21] C.W. Tang, Two-layer organic photovoltaic cell, *Appl. Phys. Lett.* 48 (1986) 183–185.
- [22] N.S. Sariciftci, L. Smilowitz, A.J. Heeger, F. Wudl, Photoinduced electron transfer from a conducting polymer to buckminsterfullerene, *Science* 258 (1992) 1474–1476.
- [23] N.S. Sariciftci, D. Braun, C. Zhang, V.I. Srdanov, A.J. Heeger, G. Stucky, F. Wudl, Semiconducting polymer–buckminsterfullerene heterojunctions: diodes, photodiodes, and photovoltaic cells, *Appl. Phys. Lett.* 62 (1993) 585–587.
- [24] G. Yu, A.J. Heeger, Charge separation and photovoltaic conversion in polymer composites with internal donor/acceptor heterojunctions, *J. Appl. Phys.* 78 (1995) 4510–4515.
- [25] J.J.M. Halls, C.A. Walsh, N.C. Greenham, E.A. Marseglia, R.H. Friend, S.C. Moratti, A.B. Holmes, Efficient photodiodes from interpenetrating polymer networks, *Nature* 376 (1995) 498–500.
- [26] G. Yu, J. Gao, J.C. Hummelen, F. Wudl, A.J. Heeger, Polymer photovoltaic cells: enhanced efficiencies via a network of internal donor–acceptor heterojunctions, *Science* 270 (1995) 1789–1791.
- [27] G. Yu, K. Pakbaz, A.J. Heeger, Semiconducting polymer diodes: large size, low cost photodetectors with excellent visible-ultraviolet sensitivity, *Appl. Phys. Lett.* 64 (1994) 3422–3424.
- [28] J.C. Hummelen, B.W. Knight, F. LePeq, F. Wudl, J. Yao, C.L. Wilkins, Preparation and characterization of fulleroid and methanofullerene derivatives, *J. Org. Chem.* 60 (1995) 532–538.
- [29] S.E. Shaheen, C.J. Brabec, N.S. Sariciftci, F. Padinger, T. Fromherz, J.C. Hummelen, 2.5% efficient organic plastic solar cells, *Appl. Phys. Lett.* 78 (2001) 841–843.
- [30] C.J. Brabec, S.E. Shaheen, C. Winder, N.S. Sariciftci, P. Denk, Effect of LiF/metal electrodes on the performance of plastic solar cells, *Appl. Phys. Lett.* 80 (2002) 1288–1290.
- [31] E. Bundgaard, F.C. Krebs, Low band gap polymers for organic photovoltaics, *Sol. Energy Mater. Sol. Cells* 91 (2007) 954–985.
- [32] Y.-J. Cheng, S.-H. Yang, C.-S. Hsu, Synthesis of conjugated polymers for organic solar cell applications, *Chem. Rev.* 109 (2009) 5868–5923.
- [33] M.T. Dang, L. Hirsch, G. Wantz, P3HT:PCBM, best seller in polymer photovoltaic research, *Adv. Mater.* 23 (2011) 3597–3602.
- [34] Y. Kim, S. Cook, S.M. Tuladhar, S.A. Choulis, J. Nelson, J.R. Durrant, D.D.C. Bradley, M. Giles, I. McCulloch, C.-S. Ha, M. Ree, A strong regioregularity effect in self-organizing conjugated polymer films and high-efficiency polythiophene:fullerene solar cells, *Nat. Mater.* 5 (2006) 197–203.
- [35] F.C. Krebs, H. Spanggaard, T. Kjær, M. Biancardo, J. Alstrup, Large area plastic solar cell modules, *Mater. Sci. Eng., B* 138 (2007) 106–111.
- [36] F.C. Krebs, M. Biancardo, B. Winther-Jensen, H. Spanggaard, J. Alstrup, Strategies for incorporation of polymer photovoltaics into garments and textiles, *Sol. Energy Mater. Sol. Cells* 90 (2006) 1058–1067.
- [37] H. Bronstein, M. Hurlangee, E.C. Fregoso, D. Beatrup, Y.W. Soon, Z. Huang, A. Hadipour, P.S. Tuladhar, S. Rossbauer, E.-H. Sohn, S. Shoaee, S.D. Dimitrov, J.M. Frost, R.S. Ashraf, T. Kirchartz, S.E. Watkins, K. Song, T. Anthopoulos, J. Nelson, B.P. Rand, J.R. Durrant, I. McCulloch, Isostructural, deeper highest occupied molecular orbital analogues of poly(3-hexylthiophene) for high-open circuit voltage organic solar cells, *Chem. Mater.* 25 (2013) 4239–4249.
- [38] Y. Sun, C.J. Takacs, S.R. Cowan, J.H. Seo, X. Gong, A. Roy, A.J. Heeger, Efficient, air-stable bulk heterojunction polymer solar cells using MoOx as the anode interfacial layer, *Adv. Mater.* 23 (2011) 2226–2230.
- [39] S. Beaupre, M. Leclerc, PCDTBT: en route for low cost plastic solar cells, *J. Mater. Chem. A* 1 (2013) 11097–11105.
- [40] T.L. Nguyen, H. Choi, S.J. Ko, M.A. Uddin, B. Walker, S. Yum, J.E. Jeong, M.H. Yun, T.J. Shin, S. Hwang, J.Y. Kim, H.Y. Woo, Semi-crystalline photovoltaic polymers with efficiency exceeding 9% in a [similar]300 nm thick conventional single-cell device, *Energy Environ. Sci.* 7 (2014) 3040–3051.
- [41] J.C. Bijleveld, V.S. Gevaerts, D. Di Nuzzo, M. Turbiez, S.G.J. Mathijssen, D.M. de Leeuw, M.M. Wienk, R.A.J. Janssen, Efficient solar cells based on an easily accessible diketopyrrolopyrrole polymer, *Adv. Mater.* 22 (2010) E242–E246.
- [42] H. Bronstein, Z. Chen, R.S. Ashraf, W. Zhang, J. Du, J.R. Durrant, P. Shukya Tuladhar, K. Song, S.E. Watkins, Y. Geerts, M.M. Wienk, R.A.J. Janssen, T. Anthopoulos, H. Sirringhaus, M. Heeney, I. McCulloch, Thieno[3,2-b]thiophene-diketopyrrolopyrrole-containing polymers for high-performance organic field-effect transistors and organic photovoltaic devices, *J. Am. Chem. Soc.* 133 (2011) 3272–3275.
- [43] Y. Liang, Y. Wu, D. Feng, S.-T. Tsai, H.-J. Son, G. Li, L. Yu, Development of new semiconducting polymers for high performance solar cells, *J. Am. Chem. Soc.* 131 (2008) 56–57.
- [44] Y. Liang, D. Feng, Y. Wu, S.-T. Tsai, G. Li, C. Ray, L. Yu, Highly efficient solar cell polymers developed via fine-tuning of structural and electronic properties, *J. Am. Chem. Soc.* 131 (2009) 7792–7799.
- [45] L. Ye, S. Zhang, W. Zhao, H. Yao, J. Hou, Highly efficient 2D-conjugated benzodithiophene-based photovoltaic polymer with linear alkylthio side chain, *Chem. Mater.* 26 (2014) 3603–3605.
- [46] X. Guo, M. Zhang, J. Tan, S. Zhang, L. Huo, W. Hu, Y. Li, J. Hou, Influence of D/A ratio on photovoltaic performance of a highly efficient polymer solar cell system, *Adv. Mater.* 24 (2012) 6536–6541.
- [47] N. Blouin, A. Michaud, M. Leclerc, A low-bandgap poly(2,7-carbazole) derivative for use in high-performance solar cells, *Adv. Mater.* 19 (2007) 2295–2300.
- [48] N. Blouin, A. Michaud, D. Gendron, S. Wakim, E. Blair, R. Neagu-Plesu, M. Belletête, G. Durocher, Y. Tao, M. Leclerc, Toward a rational design of poly(2,7-carbazole) derivatives for solar cells, *J. Am. Chem. Soc.* 130 (2008) 732–742.
- [49] S. Alem, T.-Y. Chu, S.C. Tse, S. Wakim, J. Lu, R. Movileanu, Y. Tao, F. Bélanger, D. Désilets, S. Beaupré, M. Leclerc, S. Rodman, D. Waller, R. Gaudiana, Effect of mixed solvents on PCDTBT:PC70BM based solar cells, *Org. Electron.* 12 (2011) 1788–1793.
- [50] S.H. Park, A. Roy, S. Beaupre, S. Cho, N. Coates, J.S. Moon, D. Moses, M. Leclerc, K. Lee, A.J. Heeger, Bulk heterojunction solar cells with internal quantum efficiency approaching 100%, *Nat. Photon.* 3 (2009) 297–302.
- [51] J.S. Moon, J. Jo, A.J. Heeger, Nanomorphology of PCDTBT:PC70BM bulk heterojunction solar cells, *Adv. Energy Mater.* 2 (2012) 304–308.
- [52] D.H. Wang, J.K. Kim, J.H. Seo, I. Park, B.H. Hong, J.H. Park, A.J. Heeger, Transferable graphene oxide by stamping nanotechnology: electron-transport layer for efficient bulk-heterojunction solar cells, *Angew. Chem. Int. Ed.* 52 (2013) 2874–2880.
- [53] J. Peet, J.Y. Kim, N.E. Coates, W.L. Ma, D. Moses, A.J. Heeger, G.C. Bazan, Efficiency enhancement in low-bandgap polymer solar cells by processing with alkane dithiols, *Nat. Mater.* 6 (2007) 497–500.
- [54] S. Albrecht, S. Janietz, W. Schindler, J. Frisch, J. Kurpiers, J. Kniepert, S. Inal, P. Pingel, K. Fostiropoulos, N. Koch, D. Neher, Fluorinated copolymer PCPDTBT with enhanced open-circuit voltage and reduced recombination for highly efficient polymer solar cells, *J. Am. Chem. Soc.* 134 (2012) 14932–14944.
- [55] L. Dou, C.-C. Chen, K. Yoshimura, K. Ohya, W.-H. Chang, J. Gao, Y. Liu, E. Richard, Y. Yang, Synthesis of 5H-dithieno[3,2-b:2',3'-d]pyrro as an electron-rich building block for donor–acceptor type low-bandgap polymers, *Macromolecules* 46 (2013) 3384–3390.

- [56] M.M. Wienk, M. Turbiez, J. Gilot, R.A.J. Janssen, Narrow-bandgap diketopyrrolo-pyrrole polymer solar cells: the effect of processing on the performance, *Adv. Mater.* 20 (2008) 2556–2560.
- [57] B. Walker, A.B. Tamayo, X.-D. Dang, P. Zalar, J.H. Seo, A. Garcia, M. Tantiwiwat, T.-Q. Nguyen, Nanoscale phase separation and high photovoltaic efficiency in solution-processed, small-molecule bulk heterojunction solar cells, *Adv. Funct. Mater.* 19 (2009) 3063–3069.
- [58] L. Huo, J. Hou, H.-Y. Chen, S. Zhang, Y. Jiang, T.L. Chen, Y. Yang, Bandgap and molecular level control of the low-bandgap polymers based on 3,6-dithiophen-2-yl-2,5-dihydropyrrolo[3,4-c]pyrrole-1,4-dione toward highly efficient polymer solar cells, *Macromolecules* 42 (2009) 6564–6571.
- [59] J. Jo, D. Gendron, A. Najari, J.S. Moon, S. Cho, M. Leclerc, A.J. Heeger, Bulk heterojunction solar cells based on a low-bandgap carbazole-diketopyrrolopyrrole copolymer, *Appl. Phys. Lett.* 97 (2010).
- [60] J. Ajuria, S. Chavhan, R. Tena-Zaera, J. Chen, A.J. Rondinone, P. Sonar, A. Dodabalapur, R. Pacios, Nanomorphology influence on the light conversion mechanisms in highly efficient diketopyrrolopyrrole based organic solar cells, *Org. Electron.* 14 (2013) 326–334.
- [61] J. Li, K.-H. Ong, P. Sonar, S.-L. Lim, G.-M. Ng, H.-K. Wong, H.-S. Tan, Z.-K. Chen, Design and modification of three-component randomly incorporated copolymers for high performance organic photovoltaic applications, *Polym. Chem.* 4 (2013) 804–811.
- [62] H. Bronstein, E. Collado-Fregoso, A. Hadipour, Y.W. Soon, Z. Huang, S.D. Dimitrov, R.S. Ashraf, B.P. Rand, S.E. Watkins, P.S. Tuladhar, I. Meager, J.R. Durrant, I. McCulloch, Thieno[3,2-b]thiophene-diketopyrrolopyrrole containing polymers for inverted solar cells devices with high short circuit currents, *Adv. Funct. Mater.* 23 (2013) 5647–5654.
- [63] J.W. Jung, F. Liu, T.P. Russell, W.H. Jo, A high mobility conjugated polymer based on dithienothiophene and diketopyrrolopyrrole for organic photovoltaics, *Energy Environ. Sci.* 5 (2012) 6857–6861.
- [64] K.H. Hendriks, G.H.L. Heintges, V.S. Gevaerts, M.M. Wienk, R.A.J. Janssen, High-molecular-weight regular alternating diketopyrrolopyrrole-based terpolymers for efficient organic solar cells, *Angew. Chem. Int. Ed.* 52 (2013) 8341–8344.
- [65] I. Meager, R.S. Ashraf, S. Mollinger, B.C. Schroeder, H. Bronstein, D. Beatrup, M.S. Vezie, T. Kirchartz, A. Salles, J. Nelson, I. McCulloch, Photocurrent enhancement from diketopyrrolopyrrole polymer solar cells through alkyl-chain branching point manipulation, *J. Am. Chem. Soc.* 135 (2013) 11537–11540.
- [66] Y. Liang, Y. Wu, D. Feng, S.-T. Tsai, H.-J. Son, G. Li, L. Yu, Development of new semiconducting polymers for high performance solar cells, *J. Am. Chem. Soc.* 131 (2009) 56–57.
- [67] Y. Liang, Z. Xu, J. Xia, S.-T. Tsai, Y. Wu, G. Li, C. Ray, L. Yu, For the bright future—bulk heterojunction polymer solar cells with power conversion efficiency of 7.4%, *Adv. Mater.* 22 (2010) E135–E138.
- [68] Z. He, C. Zhong, X. Huang, W.-Y. Wong, H. Wu, L. Chen, S. Su, Y. Cao, Simultaneous enhancement of open-circuit voltage, short-circuit current density, and fill factor in polymer solar cells, *Adv. Mater.* 23 (2011) 4636–4643.
- [69] Z. He, C. Zhong, S. Su, M. Xu, H. Wu, Y. Cao, Enhanced power-conversion efficiency in polymer solar cells using an inverted device structure, *Nat. Photon.* 6 (2012) 591–595.
- [70] J.-D. Chen, C. Cui, Y.-Q. Li, L. Zhou, Q.-D. Ou, C. Li, Y. Li, J.-X. Tang, Single-junction polymer solar cells exceeding 10% power conversion efficiency, *Adv. Mater.* (2014) n/a–n/a.
- [71] L. Huo, S. Zhang, X. Guo, F. Xu, Y. Li, J. Hou, Replacing alkoxy groups with alkylthienyl groups: a feasible approach to improve the properties of photovoltaic polymers, *Angew. Chem. Int. Ed.* 50 (2011) 9697–9702.
- [72] P. Adhikary, S. Venkatesan, N. Adhikari, P.P. Maharjan, O. Adebajo, J. Chen, Q. Qiao, Enhanced charge transport and photovoltaic performance of PBDTTT-C-T/PC70BM solar cells via UV-ozone treatment, *Nanoscale* 5 (2013) 10007–10013.
- [73] C. Cabanetos, A. El Labban, J.A. Bartelt, J.D. Douglas, W.R. Mateker, J.M.J. Fréchet, M.D. McGehee, P.M. Beaujuge, Linear side chains in benzo[1,2-b:4,5-b']dithiophene-thieno[3,4-c]pyrrole-4,6-dione polymers direct self-assembly and solar cell performance, *J. Am. Chem. Soc.* 135 (2013) 4656–4659.
- [74] Y.-C. Chen, C.-Y. Yu, Y.-L. Fan, L.-I. Hung, C.-P. Chen, C. Ting, Low-bandgap conjugated polymer for high efficient photovoltaic applications, *Chem. Commun.* 46 (2010) 6503–6505.
- [75] Y. Zhang, J. Zou, H.-L. Yip, K.-S. Chen, D.F. Zeigler, Y. Sun, A.K.Y. Jen, Indacenodithiophene and quinoxaline-based conjugated polymers for highly efficient polymer solar cells, *Chem. Mater.* 23 (2011) 2289–2291.
- [76] C.-P. Chen, Y.-C. Chen, C.-Y. Yu, Increased open circuit voltage in a fluorinated quinoxaline-based alternating conjugated polymer, *Polym. Chem.* 4 (2013) 1161–1166.
- [77] C.-P. Chen, H.-L. Hsu, Increasing the open-circuit voltage in high-performance organic photovoltaic devices through conformational twisting of an indacenodithiophene-based conjugated polymer, *Macromol. Rapid Commun.* 34 (2013) 1623–1628.
- [78] Z. Fei, R.S. Ashraf, Z. Huang, J. Smith, R.J. Kline, P. D'Angelo, T.D. Anthopoulos, J.R. Durrant, I. McCulloch, M. Heeney, Germaindacenodithiophene based low band gap polymers for organic solar cells, *Chem. Commun.* 48 (2012) 2955–2957.
- [79] R. Pacios, D.D.C. Bradley, Charge separation in polyfluorene composites with internal donor/acceptor heterojunctions, *Synth. Met.* 127 (2002) 261–265.
- [80] H.J. Snaith, A.C. Arias, A.C. Morteau, C. Silva, R.H. Friend, Charge generation kinetics and transport mechanisms in blended polyfluorene photovoltaic devices, *Nano Lett.* 2 (2002) 1353–1357.
- [81] Y.-C. Huang, C.-S. Tsao, C.-M. Chuang, C.-H. Lee, F.-H. Hsu, H.-C. Cha, C.-Y. Chen, T.-H. Lin, C.-J. Su, U.S. Jeng, W.-F. Su, Small- and wide-angle X-ray scattering characterization of bulk heterojunction polymer solar cells with different fullerene derivatives, *J. Phys. Chem. C* 116 (2012) 10238–10244.
- [82] Y. He, H.-Y. Chen, J. Hou, Y. Li, Indene-C60 bisadduct: a new acceptor for high-performance polymer solar cells, *J. Am. Chem. Soc.* 132 (2010) 1377–1382.
- [83] G. Zhao, Y. He, Y. Li, 6.5% Efficiency of polymer solar cells based on poly(3-hexylthiophene) and indene-C60 bisadduct by device optimization, *Adv. Mater.* 22 (2010) 4355–4358.
- [84] Y.-J. Cheng, C.-H. Hsieh, Y. He, C.-S. Hsu, Y. Li, Combination of indene-C60 bis-adduct and cross-linked fullerene interlayer leading to highly efficient inverted polymer solar cells, *J. Am. Chem. Soc.* 132 (2010) 17381–17383.
- [85] H.J. Bolink, E. Coronado, A. Forment-Alia, M. Lenes, A. La Rosa, S. Filippone, N. Martin, Polymer solar cells based on diphenylmethanofullerenes with reduced sidechain length, *J. Mater. Chem.* 21 (2011) 1382–1386.
- [86] Y.-J. Cheng, M.-H. Liao, C.-Y. Chang, W.-S. Kao, C.-E. Wu, C.-S. Hsu, Di(4-methylphenyl)methano-C60 bis-adduct for efficient and stable organic photovoltaics with enhanced open-circuit voltage, *Chem. Mater.* 23 (2011) 4056–4062.
- [87] R.B. Ross, C.M. Cardona, D.M. Guldi, S.G. Sankaranarayanan, M.O. Reese, N. Kopidakis, J. Peet, B. Walker, G.C. Bazan, E. Van Keuren, B.C. Holloway, M. Drees, Endohedral fullerenes for organic photovoltaic devices, *Nat. Mater.* 8 (2009) 208–212.
- [88] R.B. Ross, C.M. Cardona, F.B. Swain, D.M. Guldi, S.G. Sankaranarayanan, E. Van Keuren, B.C. Holloway, M. Drees, Tuning conversion efficiency in metallo endohedral fullerene-based organic photovoltaic devices, *Adv. Funct. Mater.* 19 (2009) 2332–2337.
- [89] Y. Zhou, T. Kurosawa, W. Ma, Y. Guo, L. Fang, K. Vandewal, Y. Diao, C. Wang, Q. Yan, J. Reinspach, J. Mei, A.L. Appleton, G.I. Koleilat, Y. Gao, S.C.B. Mannsfeld, A. Salles, H. Ade, D. Zhao, Z. Bao, High performance all-polymer solar cell via polymer side-chain engineering, *Adv. Mater.* 26 (2014) 3767–3772.
- [90] Y. Kim, E. Lim, Development of polymer acceptors for organic photovoltaic cells, *Polymers* 6 (2014) 382–407.
- [91] W. Li, W.S.C. Roelofs, M. Turbiez, M.M. Wienk, R.A.J. Janssen, Polymer solar cells with diketopyrrolopyrrole conjugated polymers as the electron donor and electron acceptor, *Adv. Mater.* 26 (2014) 3304–3309.
- [92] T. Earmme, Y.-J. Hwang, N.M. Murari, S. Subramaniam, S.A. Jenekhe, All-polymer solar cells with 3.3% efficiency based on naphthalene diimide-selenophene copolymer acceptor, *J. Am. Chem. Soc.* 135 (2013) 14960–14963.
- [93] W. Zhou, Z.-G. Zhang, L. Ma, Y. Li, X. Zhan, Dithienocoronene diimide based conjugated polymers as electron acceptors for all-polymer solar cells, *Sol. Energy Mater. Sol. Cells* 112 (2013) 13–19.
- [94] D. Mori, H. Bente, I. Okada, H. Ohkita, S. Ito, Highly efficient charge-carrier generation and collection in polymer/polymer blend solar cells with a power conversion efficiency of 5.7%, *Energy Environ. Sci.* 7 (2014) 2939–2943.
- [95] T.V. Pho, F.M. Toma, B.J. Tremolet de Villers, S. Wang, N.D. Treat, N.D. Eisenmenger, G.M. Su, R.C. Coffin, J.D. Douglas, J.M.J. Fréchet, G.C. Bazan, F. Wudl, M.L. Chabiniy, Decacyclene triimides: paving the road to universal non-fullerene acceptors for organic photovoltaics, *Adv. Energy Mater.* 4 (2014) n/a–n/a.
- [96] H. Hoppe, M. Niggemann, C. Winder, J. Kraut, R. Hiesgen, A. Hinsch, D. Meissner, N.S. Sariciftci, Nanoscale morphology of conjugated

- polymer/fullerene-based bulk-heterojunction solar cells, *Adv. Funct. Mater.* 14 (2004) 1005–1011.
- [97] T. Salim, L.H. Wong, B. Brauer, R. Kukreja, Y.L. Foo, Z. Bao, Y.M. Lam, Solvent additives and their effects on blend morphologies of bulk heterojunctions, *J. Mater. Chem.* 21 (2011) 242–250.
 - [98] J. Peet, C. Soci, R.C. Coffin, T.Q. Nguyen, A. Mikhailovsky, D. Moses, G.C. Bazan, Method for increasing the photoconductive response in conjugated polymer/fullerene composites, *Appl. Phys. Lett.* 89 (2006) 252105.
 - [99] N.E. Coates, I.-W. Hwang, J. Peet, G.C. Bazan, D. Moses, A.J. Heeger, 1,8-Octanedithiol as a processing additive for bulk heterojunction materials: enhanced photoconductive response, *Appl. Phys. Lett.* 93 (2008).
 - [100] Y. Zhang, Z. Li, S. Wakim, S. Alem, S.-W. Tsang, J. Lu, J. Ding, Y. Tao, Bulk heterojunction solar cells based on a new low-band-gap polymer: morphology and performance, *Org. Electron.* 12 (2011) 1211–1215.
 - [101] H. Zhou, Y. Zhang, J. Seifert, S.D. Collins, C. Luo, G.C. Bazan, T.-Q. Nguyen, A.J. Heeger, High-efficiency polymer solar cells enhanced by solvent treatment, *Adv. Mater.* 25 (2013) 1646–1652.
 - [102] W. Li, K.H. Hendriks, W.S.C. Roelofs, Y. Kim, M.M. Wienk, R.A.J. Janssen, Efficient small bandgap polymer solar cells with high fill factors for 300 nm thick films, *Adv. Mater.* 25 (2013) 3182–3186.
 - [103] F. Zhang, K.G. Jespersen, C. Björström, M. Svensson, M.R. Andersson, V. Sundström, K. Magnusson, E. Moons, A. Yartsev, O. Inganäs, Influence of solvent mixing on the morphology and performance of solar cells based on polyfluorene copolymer/fullerene blends, *Adv. Funct. Mater.* 16 (2006) 667–674.
 - [104] F.-C. Chen, H.-C. Tseng, C.-J. Ko, Solvent mixtures for improving device efficiency of polymer photovoltaic devices, *Appl. Phys. Lett.* 92 (2008).
 - [105] A.J. Moulé, K. Meerholz, Controlling morphology in polymer-fullerene mixtures, *Adv. Mater.* 20 (2008) 240–245.
 - [106] J. Lee, S.B. Jo, M. Kim, H.G. Kim, J. Shin, H. Kim, K. Cho, Donor-acceptor alternating copolymer nanowires for highly efficient organic solar cells, *Adv. Mater.* (2014) n/a–n/a.
 - [107] S. Zhang, L. Ye, W. Zhao, D. Liu, H. Yao, J. Hou, Side chain selection for designing highly efficient photovoltaic polymers with 2D-conjugated structure, *Macromolecules* 47 (2014) 4653–4659.
 - [108] C. Cabanetos, A. El Labban, J.A. Bartelt, J.D. Douglas, W.R. Mateker, J.M.J. Fréchet, M.D. McGehee, P.M. Beaujuge, Linear side chains in benzo[1,2-b:4,5-b']dithiophene-thieno[3,4-c]pyrrole-4,6-dione polymers direct self-assembly and solar cell performance, *J. Am. Chem. Soc.* 135 (2013) 4656–4659.
 - [109] A.T. Yiu, P.M. Beaujuge, O.P. Lee, C.H. Woo, M.F. Toney, J.M.J. Fréchet, Side-chain tunability of furan-containing low-band-gap polymers provides control of structural order in efficient solar cells, *J. Am. Chem. Soc.* 134 (2011) 2180–2185.
 - [110] W. Li, K.H. Hendriks, A. Furlan, W.S.C. Roelofs, M.M. Wienk, R.A.J. Janssen, Universal correlation between fibril width and quantum efficiency in diketopyrrolopyrrole-based polymer solar cells, *J. Am. Chem. Soc.* 135 (2013) 18942–18948.
 - [111] W. Li, K.H. Hendriks, A. Furlan, W.S.C. Roelofs, S.C.J. Meskers, M.M. Wienk, R.A.J. Janssen, Effect of the fibrillar microstructure on the efficiency of high molecular weight diketopyrrolopyrrole-based polymer solar cells, *Adv. Mater.* 26 (2014) 1565–1570.
 - [112] J. Ajuria, Hybrid Photovoltaic Devices Based on Organic Semiconducting Polymers and Inorganic Nanostructured Electrodes, PhD thesis, Euskal Herriko Unibertsitatea (UPV/EHU), 2012.
 - [113] Z. Bao, A. Dodabalapur, A.J. Lovinger, Soluble and processable regioregular poly(3-hexylthiophene) for thin film field-effect transistor applications with high mobility, *Appl. Phys. Lett.* 69 (1996) 4108–4110.
 - [114] H. Sirringhaus, P.J. Brown, R.H. Friend, M.M. Nielsen, K. Bechgaard, B.M.W. Langeveld-Voss, A.J.H. Spiering, R.A.J. Janssen, E.W. Meijer, P. Herwig, D.M. de Leeuw, Two-dimensional charge transport in self-organized, high-mobility conjugated polymers, *Nature* 401 (1999) 685–688.
 - [115] I. Burgués-Ceballos, M. Campoy-Quiles, L. Francesch, P.D. Lacharmoise, Fast annealing and patterning of polymer solar cells by means of vapor printing, *J. Polym. Sci., Part B: Polym. Phys.* 50 (2012) 1245–1252.
 - [116] D. Nassyrov, C. Muller, A. Roige, I. Burgués-Ceballos, J. Oriol Osso, D.B. Amabilino, M. Garriga, M. Isabel Alonso, A.R. Goni, M. Campoy-Quiles, Vapour printing: patterning of the optical and electrical properties of organic semiconductors in one simple step, *J. Mater. Chem.* 22 (2012) 4519–4526.
 - [117] T.M. Brown, R.H. Friend, I.S. Millard, D.J. Lacey, J.H. Burroughes, F. Cacialli, LiF/Al cathodes and the effect of LiF thickness on the device characteristics and built-in potential of polymer light-emitting diodes, *Appl. Phys. Lett.* 77 (2000) 3096–3098.
 - [118] T.M. Brown, J.S. Kim, R.H. Friend, F. Cacialli, R. Daik, W.J. Feast, Built-in field electroabsorption spectroscopy of polymer light-emitting diodes incorporating a doped poly(3,4-ethylene dioxthiophene) hole injection layer, *Appl. Phys. Lett.* 75 (1999) 1679–1681.
 - [119] L. Groenendaal, F. Jonas, D. Freitag, H. Pielartzik, J.R. Reynolds, Poly(3,4-ethylenedioxythiophene) and its derivatives: past, present, and future, *Adv. Mater.* 12 (2000) 481–494.
 - [120] A. Martínez-Otero, X. Elias, R. Betancur, J. Martorell, High-performance polymer solar cells using an optically enhanced architecture, *Adv. Opt. Mater.* 1 (2013) 37–42.
 - [121] M. Campoy-Quiles, T. Ferenczi, T. Agostinelli, P.G. Etchegoin, Y. Kim, T.D. Anthopoulos, P.N. Stavrinou, D.D.C. Bradley, J. Nelson, Morphology evolution via self-organization and lateral and vertical diffusion in polymer:fullerene solar cell blends, *Nat. Mater.* 7 (2008) 158–164.
 - [122] L.M. Chen, Z. Hong, G. Li, Y. Yang, Recent progress in polymer solar cells: manipulation of polymer: fullerene morphology and the formation of efficient inverted polymer solar cells, *Adv. Mater.* 21 (2009) 1434–1449.
 - [123] K. Sugiyama, H. Ishii, Y. Ouchi, K. Seki, Dependence of indium-tin-oxide work function on surface cleaning method as studied by ultraviolet and X-ray photoemission spectroscopies, *J. Appl. Phys.* 87 (2000) 295–298.
 - [124] A.C. Arias, M. Granström, D.S. Thomas, K. Petritsch, R.H. Friend, Doped conducting-polymer-semiconducting-polymer interfaces: their use in organic photovoltaic devices, *Phys. Rev. B* 60 (1999) 1854–1860.
 - [125] A.J. Campbell, D.D.C. Bradley, H. Antoniadis, M. Inbasekaran, W.W. Wu, E.P. Woo, Transient and steady-state space-charge-limited currents in polyfluorene copolymer diode structures with ohmic hole injecting contacts, *Appl. Phys. Lett.* 76 (2000) 1734–1736.
 - [126] V. Shrotriya, G. Li, Y. Yao, C.-W. Chu, Y. Yang, Transition metal oxides as the buffer layer for polymer photovoltaic cells, *Appl. Phys. Lett.* 88 (2006).
 - [127] M.D. Irwin, D.B. Buchholz, A.W. Hains, R.P.H. Chang, T.J. Marks, P-Type semiconducting nickel oxide as an efficiency-enhancing anode interfacial layer in polymer bulk-heterojunction solar cells, *Proc. Natl. Acad. Sci.* 105 (2008) 2783–2787.
 - [128] E.I. Haskal, A. Curioni, P.F. Seidler, W. Andreoni, Lithium–aluminum contacts for organic light-emitting devices, *Appl. Phys. Lett.* 71 (1997) 1151–1153.
 - [129] L.S. Hung, C.W. Tang, M.G. Mason, Enhanced electron injection in organic electroluminescence devices using an Al/LiF electrode, *Appl. Phys. Lett.* 70 (1997) 152–154.
 - [130] J. Zhi-Qiang, W. Xiao-Ming, H. Yu-Lin, D. Mu-Sen, S. Yue-Ju, S. Li-Ying, Y. Shou-Gen, Improving efficiency of organic light-emitting devices by optimizing the LiF interlayer in the hole transport layer, *Chin. Phys. B* 20 (2011) 107803.
 - [131] X. Jiang, H. Xu, L. Yang, M. Shi, M. Wang, H. Chen, Effect of CsF interlayer on the performance of polymer bulk heterojunction solar cells, *Sol. Energy Mater. Sol. Cells* 93 (2009) 650–653.
 - [132] M. Reinhard, J. Hanisch, Z. Zhang, E. Ahlswede, A. Colmann, U. Lemmer, Inverted organic solar cells comprising a solution-processed cesium fluoride interlayer, *Appl. Phys. Lett.* 98 (2011).
 - [133] L. Ke, H.C. Ling, R.S. Kumar, Y. Xiao, S.J. Chua, Magnesium fluoride modified interfaces for organic light-emitting diode, *Thin Solid Films* 515 (2007) 3881–3886.
 - [134] J.Y. Kim, S.H. Kim, H.H. Lee, K. Lee, W. Ma, X. Gong, A.J. Heeger, New architecture for high-efficiency polymer photovoltaic cells using solution-based titanium oxide as an optical spacer, *Adv. Mater.* 18 (2006) 572–576.
 - [135] M.-H. Park, J.-H. Li, A. Kumar, G. Li, Y. Yang, Doping of the metal oxide nanostructure and its influence in organic electronics, *Adv. Funct. Mater.* 19 (2009) 1241–1246.
 - [136] J. Gilot, I. Barbu, M.M. Wienk, R.A.J. Janssen, The use of ZnO as optical spacer in polymer solar cells: theoretical and experimental study, *Appl. Phys. Lett.* 91 (2007) 113520.
 - [137] T. Kuwabara, M. Nakamoto, Y. Kawahara, T. Yamaguchi, K. Takahashi, Characterization of ZnS-layer-inserted bulk-heterojunction organic solar cells by ac impedance spectroscopy, *J. Appl. Phys.* 105 (2009).
 - [138] L. Jiang, A. Li, X. Deng, S. Zheng, K.-Y. Wong, Effects of cathode modification using spin-coated lithium acetate on the

- performances of polymer bulk-heterojunction solar cells, *Appl. Phys. Lett.* 102 (2013).
- [139] F.-C. Chen, J.-L. Wu, S.S. Yang, K.-H. Hsieh, W.-C. Chen, Cesium carbonate as a functional interlayer for polymer photovoltaic devices, *J. Appl. Phys.* 103 (2008).
- [140] H.-H. Liao, L.-M. Chen, Z. Xu, G. Li, Y. Yang, Highly efficient inverted polymer solar cell by low temperature annealing of Cs_2CO_3 interlayer, *Appl. Phys. Lett.* 92 (2008).
- [141] Y. Park, S. Noh, D. Lee, J. Kim, C. Lee, Study of the cesium carbonate (Cs_2CO_3) inter layer fabricated by solution process on P3HT:PCBM solar cells, *Mol. Cryst. Liq. Cryst.* 538 (2011) 20–27.
- [142] F. Huang, H. Wu, Y. Cao, Water/alcohol soluble conjugated polymers as highly efficient electron transporting/injection layer in optoelectronic devices, *Chem. Soc. Rev.* 39 (2010) 2500–2521.
- [143] K. Sun, B. Zhao, A. Kumar, K. Zeng, J. Ouyang, Inverted polymer solar cells with indium tin oxide modified with solution-processed zwitterions as the transparent cathode, *ACS Appl. Mater. Interfaces* 4 (2012) 2009–2017.
- [144] K. Sun, B. Zhao, V. Murugesan, A. Kumar, K. Zeng, J. Subbiah, W.W.H. Wong, D.J. Jones, J. Ouyang, High-performance polymer solar cells with a conjugated zwitterion by solution processing or thermal deposition as the electron-collection interlayer, *J. Mater. Chem.* 22 (2012) 24155–24165.
- [145] T.M. Khan, Y. Zhou, A. Dindar, J.W. Shim, C. Fuentes-Hernandez, B. Kippelen, Organic photovoltaic cells with stable top metal electrodes modified with polyethylenimine, *ACS Appl. Mater. Interfaces* 6 (2014) 6202–6207.
- [146] C.-H. Hsieh, Y.-J. Cheng, P.-J. Li, C.-H. Chen, M. Dubosc, R.-M. Liang, C.-S. Hsu, Highly efficient and stable inverted polymer solar cells integrated with a cross-linked fullerene material as an interlayer, *J. Am. Chem. Soc.* 132 (2010) 4887–4893.
- [147] Q. Mei, C. Li, X. Gong, H. Lu, E. Jin, C. Du, Z. Lu, L. Jiang, X. Meng, C. Wang, Z. Bo, Enhancing the performance of polymer photovoltaic cells by using an alcohol soluble fullerene derivative as the interfacial layer, *ACS Appl. Mater. Interfaces* 5 (2013) 8076–8080.
- [148] S. van Reenen, S. Kouijzer, R.A.J. Janssen, M.M. Wienk, M. Kemerink, Origin of work function modification by ionic and amine-based interface layers, *Adv. Mater. Interfaces* 1 (2014) n/a–n/a.
- [149] J. Reinhardt, M. Grein, C. Bühler, M. Schubert, U. Würfel, Identifying the impact of surface recombination at electrodes in organic solar cells by means of electroluminescence and modeling, *Adv. Energy Mater.* (2014) n/a–n/a.
- [150] C. Duan, K. Zhang, C. Zhong, F. Huang, Y. Cao, Recent advances in water/alcohol-soluble [small pi]-conjugated materials: new materials and growing applications in solar cells, *Chem. Soc. Rev.* 42 (2013) 9071–9104.
- [151] H. Ma, H.-L. Yip, F. Huang, A.K.Y. Jen, Interface engineering for organic electronics, *Adv. Funct. Mater.* 20 (2010) 1371–1388.
- [152] A. Guerrero, N.F. Montcada, J. Ajuria, I. Etxebarria, R. Pacios, G. Garcia-Belmonte, E. Palomares, Charge carrier transport and contact selectivity limit the operation of PTB7-based organic solar cells of varying active layer thickness, *J. Mater. Chem. A* 1 (2013) 12345–12354.
- [153] A. Guerrero, B. Döring, T. Ripolles-Sanchis, M. Aghamohammadi, E. Barrena, M. Campoy-Quiles, G. Garcia-Belmonte, Interplay between fullerene surface coverage and contact selectivity of cathode interfaces in organic solar cells, *ACS Nano* 7 (2013) 4637–4646.
- [154] J. Ajuria, I. Etxebarria, W. Cambarau, U. Munecas, R. Tena-Zaera, J.C. Jimeno, R. Pacios, New designs for integration in tandem cells, top or bottom detecting devices, and photovoltaic windows, *Energy Environ. Sci.* 4 (2011) 453–458.
- [155] Y. Zhou, C. Fuentes-Hernandez, J. Shim, J. Meyer, A.J. Giordano, H. Li, P. Winget, T. Papadopoulos, H. Cheun, J. Kim, M. Fenoll, A. Dindar, W. Haske, E. Najafabadi, T.M. Khan, H. Sojoudi, S. Barlow, S. Graham, J.-L. Brédas, S.R. Marder, A. Kahn, B. Kippelen, A universal method to produce low-work function electrodes for organic electronics, *Science* 336 (2012) 327–332.
- [156] A.K.K. Kyaw, D.H. Wang, V. Gupta, J. Zhang, S. Chand, G.C. Bazan, A.J. Heeger, Efficient solution-processed small-molecule solar cells with inverted structure, *Adv. Mater.* 25 (2013) 2397–2402.
- [157] W. Shockley, H.J. Queisser, Detailed balance limit of efficiency of p-n junction solar cells, *J. Appl. Phys.* 32 (1961) 510–519.
- [158] T. Ameri, G. Dennler, C. Lungenschmied, C.J. Brabec, Organic tandem solar cells: a review, *Energy Environ. Sci.* 2 (2009) 347–363.
- [159] S. Sista, Z. Hong, L.-M. Chen, Y. Yang, Tandem polymer photovoltaic cells-current status, challenges and future outlook, *Energy Environ. Sci.* 4 (2011) 1606–1620.
- [160] J. You, L. Dou, Z. Hong, G. Li, Y. Yang, Recent trends in polymer tandem solar cells research, *Prog. Polym. Sci.* 38 (2013) 1909–1928.
- [161] S. Sista, Z. Hong, M.-H. Park, Z. Xu, Y. Yang, High-efficiency polymer tandem solar cells with three-terminal structure, *Adv. Mater.* 22 (2010) E77–E80.
- [162] I. Etxebarria, A. Furlan, J. Ajuria, F.W. Fecher, M. Voigt, C.J. Brabec, M.M. Wienk, L. Slooff, S. Veenstra, J. Gilot, R. Pacios, Series vs parallel connected organic tandem solar cells: cell performance and impact on the design and operation of functional modules, *Sol. Energy Mater. Sol. Cells* (2014).
- [163] A.D. Vos, Detailed balance limit of the efficiency of tandem solar cells, *J. Phys. D Appl. Phys.* 13 (1980) 839.
- [164] M.C. Scharber, D. Mühlbacher, M. Koppe, P. Denk, C. Waldauf, A.J. Heeger, C.J. Brabec, Design rules for donors in bulk-heterojunction solar cells—towards 10% energy-conversion efficiency, *Adv. Mater.* 18 (2006) 789–794.
- [165] G. Dennler, M.C. Scharber, T. Ameri, P. Denk, K. Forberich, C. Waldauf, C.J. Brabec, Design rules for donors in bulk-heterojunction tandem solar cells-towards 15% energy-conversion efficiency, *Adv. Mater.* 20 (2008) 579–583.
- [166] J. Gierschner, J. Cornil, H.J. Egelhaaf, Optical bandgaps of π -conjugated organic materials at the polymer limit: experiment and theory, *Adv. Mater.* 19 (2007) 173–191.
- [167] J.Y. Kim, K. Lee, N.E. Coates, D. Moses, T.-Q. Nguyen, M. Dante, A.J. Heeger, Efficient tandem polymer solar cells fabricated by all-solution processing, *Science* 317 (2007) 222–225.
- [168] V. Shrotriya, E.H.E. Wu, G. Li, Y. Yan, Y. Yang, Efficient light harvesting in multiple-device stacked structure for polymer solar cells, *Appl. Phys. Lett.* 88 (2006) 064104.
- [169] G. Dennler, H. Prall, R. Koeppe, M. Egginger, R. Autengruber, N.S. Sariciftci, Enhanced spectral coverage in tandem organic solar cells, *Appl. Phys. Lett.* 89 (2006).
- [170] A. Hadipour, B. de Boer, J. Wildeman, F.B. Kooistra, J.C. Hummelen, M.G.R. Turbiez, M.M. Wienk, R.A.J. Janssen, P.W.M. Blom, Solution-processed organic tandem solar cells, *Adv. Funct. Mater.* 16 (2006) 1897–1903.
- [171] S. Sista, M.-H. Park, Z. Hong, Y. Wu, J. Hou, W.L. Kwan, G. Li, Y. Yang, Highly efficient tandem polymer photovoltaic cells, *Adv. Mater.* 22 (2010) 380–383.
- [172] J. Yang, R. Zhu, Z. Hong, Y. He, A. Kumar, Y. Li, Y. Yang, A robust inter-connecting layer for achieving high performance tandem polymer solar cells, *Adv. Mater.* 23 (2011) 3465–3470.
- [173] L. Dou, J. You, J. Yang, C.-C. Chen, Y. He, S. Murase, T. Moriarty, K. Emery, G. Li, Y. Yang, Tandem polymer solar cells featuring a spectrally matched low-bandgap polymer, *Nat. Photon.* 6 (2012) 180–185.
- [174] J. Gilot, M.M. Wienk, R.A.J. Janssen, Optimizing polymer tandem solar cells, *Adv. Mater.* 22 (2010) E67–E71.
- [175] P.W.M. Blom, V.D. Mihailescu, L.J.A. Koster, D.E. Markov, Device Physics of polymer: fullerene bulk heterojunction solar cells, *Adv. Mater.* 19 (2007) 1551–1566.
- [176] V.S. Gevaerts, A. Furlan, M.M. Wienk, M. Turbiez, R.A.J. Janssen, Solution processed polymer tandem solar cell using efficient small and wide bandgap polymer: fullerene blends, *Adv. Mater.* 24 (2012) 2130–2134.
- [177] M. Hiramoto, M. Suezaki, M. Yokoyama, Effect of thin gold interstitial-layer on the photovoltaic properties of tandem organic solar cell, *Chem. Lett.* 19 (1990) 327–330.
- [178] A. Colmann, J. Junge, C. Kayser, U. Lemmer, Organic tandem solar cells comprising polymer and small-molecule subcells, *Appl. Phys. Lett.* 89 (2006).
- [179] A.G.F. Janssen, T. Riedl, S. Hamwi, H.H. Johannes, W. Kowalsky, Highly efficient organic tandem solar cells using an improved connecting architecture, *Appl. Phys. Lett.* 91 (2007).
- [180] D.W. Zhao, X.W. Sun, C.Y. Jiang, A.K.K. Kyaw, G.Q. Lo, D.L. Kwong, Efficient tandem organic solar cells with an Al/MoO₃ intermediate layer, *Appl. Phys. Lett.* 93 (2008).
- [181] B. Joon Lee, H. Jung Kim, W.-i. Jeong, J.-j. Kim, A transparent conducting oxide as an efficient middle electrode for flexible organic tandem solar cells, *Sol. Energy Mater. Sol. Cells* 94 (2010) 542–546.
- [182] K. Kawano, N. Ito, T. Nishimori, J. Sakai, Open circuit voltage of stacked bulk heterojunction organic solar cells, *Appl. Phys. Lett.* 88 (2006).
- [183] C.-H. Chou, W.L. Kwan, Z. Hong, L.-M. Chen, Y. Yang, A metal-oxide interconnection layer for polymer tandem solar cells with an inverted architecture, *Adv. Mater.* 23 (2010) 1282–1286.
- [184] L. Dou, J. Gao, E. Richard, J. You, C.-C. Chen, K.C. Cha, Y. He, G. Li, Y. Yang, Systematic investigation of benzodithiophene- and

- diketopyrrolopyrrole-based low-bandgap polymers designed for single junction and tandem polymer solar cells, *J. Am. Chem. Soc.* 134 (2012) 10071–10079.
- [185] J.-H. Kim, C.E. Song, B. Kim, I.-N. Kang, W.S. Shin, D.-H. Hwang, Thieno[3,2-b]thiophene-substituted benzo[1,2-b:4,5-b']dithiophene as a promising building block for low bandgap semiconducting polymers for high-performance single and tandem organic photovoltaic cells, *Chem. Mater.* 26 (2013) 1234–1242.
- [186] J. You, C.-C. Chen, Z. Hong, K. Yoshimura, K. Ohya, R. Xu, S. Ye, J. Gao, G. Li, Y. Yang, 10.2% Power conversion efficiency polymer tandem solar cells consisting of two identical sub-cells, *Adv. Mater.* 25 (2013) 3973–3978.
- [187] C.-C. Chen, W.-H. Chang, K. Yoshimura, K. Ohya, J. You, J. Gao, Z. Hong, Y. Yang, An efficient triple-junction polymer solar cell having a power conversion efficiency exceeding 11%, *Adv. Mater.* 26 (2014) 5670–5677.
- [188] A.R.B.M. Yusoff, D. Kim, H.P. Kim, F.K. Shneider, W.J. da Silva, J. Jang, A high efficiency solution processed polymer inverted triple-junction solar cell exhibiting a power conversion efficiency of 11.83%, *Energy Environ. Sci.* (2015).